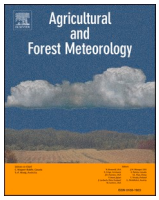
Agricultural and Forest Meteorology 339 (2023) 109588



Contents lists available at ScienceDirect

Agricultural and Forest Meteorology

journal homepage: www.elsevier.com/locate/agrformet



The effects of forest composition and management on evapotranspiration in the New Jersey Pinelands

Bernard N. Isaacson [a,b,c,*], Yun Yang [d], Martha C. Anderson [e], Kenneth L. Clark [f], Jason C. Grabosky [c]

[a] USDA Forest Service, Southern Research Station, Forest Inventory and Analysis, 4700 Old Kingston Pike, Knoxville, TN, 37919, USA
[b] New Jersey Forest Service, New Jersey Department of Environmental Protection, 501 E. State Street, Trenton, NJ, 08625, USA
[c] Department of Ecology, Evolution, and Natural Resources, Rutgers University, 14 College Farm Road, New Brunswick, NJ, 08901, USA
[d] Department of Forestry, Mississippi State University, Mississippi State, MS, 39762, USA
[e] USDA ARS, Hydrology and Remote Sensing Laboratory, 10300 Baltimore Avenue, Building 003, BARC-West, Beltsville, MD, USA
[f] USDA Forest Service, Northern Research Station, Silas Little Experimental Forest, 501 Four Mile Road, New Lisbon, NJ, 08064, USA

ARTICLE INFO

Keywords:
Evapotranspiration
Forest
Remote sensing
Data fusion
Management
Water yield

ABSTRACT

Forests deliver contrasting ecosystem services in relation to water, both provisioning it through filtration and recharge, and consuming it through evapotranspiration. Understanding forest evapotranspiration is critical for landscapes managed in part for the social benefits of their water provisioning ecosystem services. We used the flux disaggregation algorithm for the Atmosphere-Land Exchange Inverse model (DisALEXI) with remotely sensed data to characterize landscape-scale evapotranspiration at 30-m spatial resolution over the forested coastal plain Pinelands of southern New Jersey, USA. We examined changes in evapotranspiration due to forest compositional and cover differences, then evaluated the effects of three common management actions (thinning, seed tree regeneration, and prescribed burning) on stand evapotranspiration. Among various forest compositions, upland oak forests had the lowest annual evapotranspiration, while Atlantic white cedar had the highest. In uplands, increasing proportions of conifers increased evapotranspiration, as did increased canopy cover in conifer stands. Seed tree harvests reduced evapotranspiration for about 13 years, while thinning reduced forest water use for approximately six years. Prescribed fires had variable effects, but their typical application did not reduce evapotranspiration for a complete growing season. Our research can help to inform models and decision-making around forests and landscape water yield.

1. Introduction

Forests are the dominant source of water yield across the North America (Brown et al., 2008; Sun et al., 2015) and have long been recognized for their critical role in water provisioning. Precipitation falling on a forest soil not only works its way downstream for human or ecosystem use but is also consumed by forest vegetation through evapotranspiration (ET). In the Pinelands of the southern coastal plain of New Jersey, ET is the largest component of the water budget (Clark et al., 2012; Sloto and Buxton, 2005; Walker et al., 2011, Sumner et al. 2012). Even in the densely-populated human landscape of New Jersey, forest still covers 40% of the land area (Crocker et al., 2017), so understanding forest ET is a critical component for planning around water resources.

Management of the natural resources of the Pinelands is currently dictated by multiple resource priorities at different scales of government. Federal legislation establishing the Pinelands National Reserve declared a national interest in protecting the land and water resources of the area for their 'significant ecological, natural, cultural, recreation, agricultural and public health benefits." (National Parks and Recreation Act of 1978). Numerous state laws with overlapping jurisdiction in land management articulate goals of ensuring 'adequate supply and quality of water for citizens of the State' (Water Supply Management Act, 1981), preservation of wetlands to protect drinking water supplies and maintain baseflow (Freshwater Wetlands Protection Act, 1987), preservation of habitat for rare species (New Jersey Legislature, 1961), minimization of forest fire threats to life and property, and overall management of the forest resources for long-term sustained yield, soil fertility, and water

* Corresponding author.
E-mail address: Bernard.Isaacson@usda.gov (B.N. Isaacson).

https://doi.org/10.1016/j.agrformet.2023.109588
Received 29 September 2022; Received in revised form 15 May 2023; Accepted 28 June 2023
Available online 8 July 2023
0168-1923/© 2023 Published by Elsevier B.V.

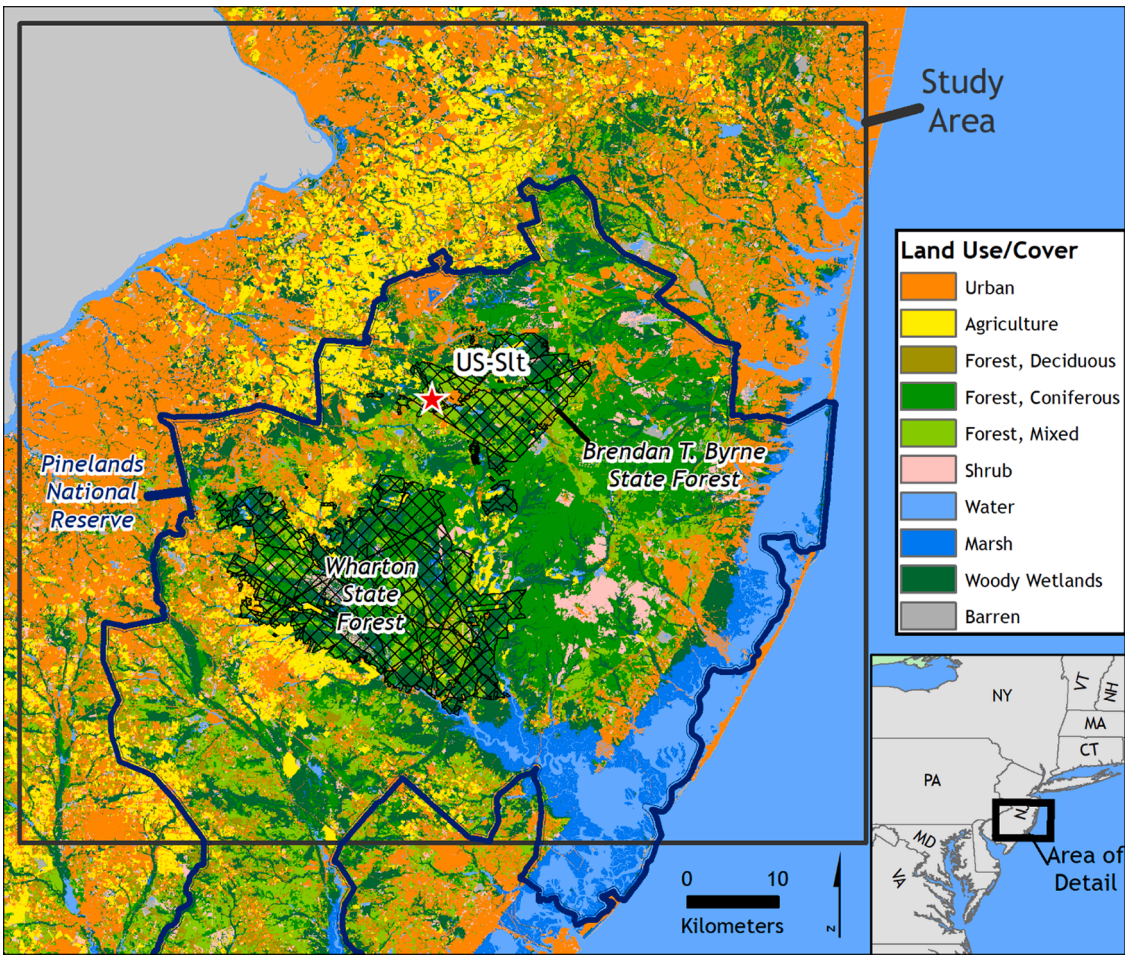


Fig. 1. DisALEXI study area and land cover as defined by the New Jersey Department of Environmental Protection's 2015 Land Use/Land Cover Dataset. Hatched area indicates state forest properties used in analysis. Red star labeled US-Slt is the location of the Silas Little Experimental Forest flux tower.

yield (State Parks and Forestry Resource Act, 1983). Many of these goals were affirmed especially for the Pinelands region through a regional development and land management authority (Pinelands Protection Act, 1979). Further, local jurisdictions also have their own objectives for the management of land within their borders, which involve permitting for all tree cutting so as to 'maintain adequate tree density', whether for conservation of natural resources (Ocean Township 1989), increasing groundwater recharge (Galloway Township 2006), maintaining water resource integrity (Jackson Township 2009), improving air quality (Galloway Township, 2006; Jackson Township, 2009), or maintaining property values (Galloway Township, 2006). Given the overlapping purview of these human factors, as well as the intersection of drivers of these natural systems themselves, management actions should ideally attempt to balance a variety of tradeoffs. For example, large-scale fuel reduction to prevent wildfire spread may conflict with local ordinances seeking to maintain tree density, while also affecting hydrologic behavior in a basin's discharge area.

Data-driven decision-making requires an understanding of the processes supporting ecosystem services. Forest hydrologists have long sought to connect forest management to water yield (Douglass and Swank, 1972), with implications for the seasonality of flow, effects of flow changes on stream habitat, and downstream human water use. Reductions in forest stand ET resulting from varying management applications are frequently observed (Bosch and Hewlett, 1982; Stednick, 1996) and have been used in predictive modeling for water yield management (Sun et al., 2016, 2015). Economic ecosystem service models that attempt to characterize tradeoffs in policy and management should be sensitive to the hydrologic behavior of different forest disturbance events (Ovando and Brouwer, 2019; Garcia-Prats et al., 2016; Simonit et al., 2015). Interest in water will be a major driver of how societies manage their forest resources in this century (Vose et al., 2011).

Tradeoffs between different observational techniques determine which method for estimating ET is appropriate. Flux towers provide measurements over a relatively small area (the "flux footprint") that are highly temporally resolved but are capital intensive. Basin gauges can cover a wider area, but they necessarily integrate over a watershed that may exist at a broader scale than the phenomenon of interest for a specific study, introducing uncertainty for some applications. Sap flux measurements can evaluate transpiration from single trees but to scale up to stand must be corrected to include the contributions of understory, interception, and evaporation (Ford et al., 2007). In contrast, remote sensing can provide fine-grained spatially-continuous information not possible with other methods. These factors make remote sensing-derived ET an attractive alternative for examination of landscape processes.

Many current remote sensing-derived ET model products provide information at coarse spatial resolution on the order of kilometers because they are based on moderate-to-coarse resolution sensors like MODIS (Running et al., 2017) or GOES (Anderson et al., 2007). These sensors provide fine-scale temporal resolution (hourly to daily) but are too spatially coarse to characterize all but the most extensive forest stands. In contrast, Landsat-scale spatial resolution (30m) provides data that can be examined at the scale of a forest patch, enabling investigation of details such as the behavior of different species, forest inventory attributes, and other fine-scale traits (Wulder et al., 2008). However, in cloudy regions the temporal resolution of Landsat (8-16 day revisit interval) may be too infrequent to capture seasonal and

management-induced changes in ET, particularly when integrating through time and between forest types with differing phenology, or for management activities with shorter effect duration.

In this study we use a data fusion method that combines the temporal characteristics of moderate resolution sensors with the fine spatial detail of Landsat to create modeled daily ET products at 30 m resolution. ET estimates from both sensor classes are obtained from the disaggregated Atmosphere-Land Exchange Inverse (DisALEXI; Anderson et al., 2004; Norman et al., 2003) surface energy balance algorithm, driven primarily by thermal-infrared remote sensing estimates of land-surface temperature. Thermal methods are particularly advantageous for ET monitoring because of their sensitivity to the relationship between transpiration, plant stress, and canopy temperature. The DisALEXI data fusion approach has been widely and successfully applied in agricultural landscapes (e.g., Anderson et al., 2018; Knipper et al., 2020; Yang et al., 2021b). In addition, this approach has been applied to managed and unmanaged forest land to study relationships between stand age and water use (Yang et al., 2017) and forest ET and mortality in response to drought at 30m resolution (Yang et al., 2020, Yang et al., 2021a), approaching the scale of individual tree canopies.

Our intent in this study is to use this ET data fusion system to provide hydrologic decision support for forest and water management in the New Jersey Pinelands, the largest forested landscape on the mid-Atlantic coastal plain. The Pinelands are a good testbed for demonstrating the value of isolating the effects of management on ET. This region is underlain by an unconfined aquifer, blanketed in forest, ostensibly managed for a balance of ecosystem services, and has a well-documented history of land use and disturbance. Here, we seek to examine how forest composition affects ET and to describe the effects of land management actions on forest ET. We hypothesize that forest ET in this area results from the interactive relationships between forest type, land cover type, and intensity of management, and investigate these relationships through a remote-sensing time-series based model of ET.

2. Materials & methods

2.1. Study area & period

The study site covers the central and northern portions of New Jersey's Coastal Plain physiographic province, within the Atlantic Coastal Pine Barrens Ecoregion (Woods et al., 2007) (Fig. 1). This area is characterized by warm, humid summers and moderately cold and occasionally snowy winters (Runkle et al., 2017). The dominant land cover is forest, much of which is jurisdictionally located within the Pinelands National Reserve. Most of the forest in the area is publicly owned (Crocker et al., 2017; Hewes et al., 2014). Thirty-year (1981-2010) mean annual precipitation for the county covering the largest portion of the study area (Burlington County) is 1148 mm. January mean temperature is 0.2 °C, and July mean temperature is 24.4 °C.

Both upland and wetland forests are dominated by yellow pine species. While pitch pine (*Pinus rigida* Mill.) is dominant, shortleaf pine (*P. chinate* Mill.), Virginia pine (*P. virginiana* Mill.), black oak (*Quercus velutina* Lam.), white oak (*Q. alba* L.), chestnut oak (*Q. prinus* L.), post oak (*Q. stellata* Wangenh.), and associated species are also found throughout the upland area. Transitional and seasonal wetlands are dominated by pitch pine, with wetter sites occupied by Atlantic white cedar (*Chamaecyparis thyoides* L.), red maple (*Acer rubrum* L.), and blackgum (*Nyssa sylvatica* Marshall). Ericaceous shrubs are extensive throughout both uplands and wetlands, with *Vaccinium* spp. and *Gaylussacia* spp. dominant.

Upland soils of the region are sandy and well- to excessively-drained, while wetlands often have a layer of peat atop sand; both uplands and lowlands are strongly- to extremely- acidic. The Kirkwood Cohansey water table aquifer underlies most of the study area. For forested subwatersheds in this region the water budget is dominated by ET, with precipitation otherwise going mainly to groundwater recharge and streamflow (Schäfer et al., 2014; Sloto and Buxton, 2005; Walker et al., 2011).

We chose to study ET for the years 2015-2018 (inclusive), as these years overlapped with the collection of ground-based forest inventory data (2017-2019), the span of available record on forest management that involved cutting (1958-2018), and prescribed burns (2000-2018), and the timing of the cover type dataset (2015). The use of 4-years of ET data allowed us to characterize a portion of the site response for an individual management activity, while the wide spatial coverage of the ET model enabled us to include a broad set of activities, substituting space for some time.

2.2. DisALEXI model & flux tower data

The ALEXI/DisALEXI modeling system are based on the Two-Source Energy Balance (TSEB) land-surface representation developed by Norman et al. (1995), which uses measurements of land surface temperature to diagnose evaporative cooling rates. The regional ALEXI model (Anderson et al., 1997) uses measurements of the morning rate of surface temperature rise typically obtained from geostationary satellites such as GOES (Geostationary Operational Environmental Satellite). Temperature observations are obtained two or more times over the morning hours and the surface flux rate is integrated over the time interval, making the model less sensitive to sensor biases in measured brightness temperature that can result from using a single observation (Anderson et al., 1997). The two-source aspect of TSEB partitions surface fluxes into vegetation and soil components, allowing separation of ET into E (soil evaporation) and T (transpiration) fluxes. ALEXI applies TSEB at a coarse spatial resolution (4 km) commensurate with the GOES thermal imager scale (4 km). Higher spatial resolution can be achieved through an ALEXI downscaling approach, DisALEXI, which applies the TSEB model to finer-scale thermal and vegetation-fraction data obtained from polar-orbiting systems like Landsat (30 m/8-16 day), MODIS or VIIRS (500 m/~daily). The ET output from DisALEXI is iteratively aggregated and compared to the broader ALEXI pixel scale and adjusted until the fine-scale fluxes are consistent with the broader-scale fluxes, ensuring that energy is conserved between spatial scales (Anderson et al., 2008). To achieve daily ET at Landsat-scale resolution, DisALEXI is run at both the MODIS (500 m, moderate-scale) and Landsat (30 m, fine-scale) scale. On dates when it is possible to run the fine-scale DisALEXI model, the paired fine-scale data and moderate-scale data are used as training sets for temporal and spatial gap filling using the Spatial and Temporal Adaptive Reflectance Fusion Model (Gao et al., 2006). The steps used here to construct 30 m resolution, daily ET timeseries over the Pinelands study domain are detailed in Yang et al. (2017).

Daily 30 m ET estimates from DisALEXI were evaluated using local flux tower data; for this study we used the Silas Little Experimental Forest flux tower data (AmeriFlux site US-Slt), operated by the USDA Forest Service within Brendan T. Byrne State Forest (Clark, 2016). We obtained these data at 30-min timesteps but for a variety of reasons there were missing observations or timesteps where methodological assumptions were violated. This is a common drawback of using eddy covariance flux data, requiring a tradeoff between excluding data and having continuous observations (Burba, 2013). While there are many alternatives for gap-filling missing observations (Moffat et al., 2007), we found that extensive gap-filling introduced additional uncertainty into the eddy covariance dataset but did not increase our ability to evaluate DisALEXI performance. Therefore, we used a relatively simple method to fill in short flux observation gaps. Collectively, relative humidity, soil conduction (G), air temperature, and net radiation (R_n) were missing for less than 0.1% of data and were filled using interpolation. For sensible heat (H) and latent energy (LE) we used linear interpolation to fill timesteps that were two-hours or shorter in duration, while gaps longer than this were flagged and not used to compare the ground data against the model outputs. We did not filter out timesteps when friction velocity (u*) was lower than 0.2 m s^{-1}, or during periods of light precipitation, as

Table 1
Inventory plot characteristics by plot type grouping. Means are shown with standard deviations in parenthesis.

Forest type	# of Plots	Basal area, m^2 ha^{-1}	Trees per hectare	Stand density index, SDI	Relative Density Index, SDI/SDI_{max}	Quadratic mean DBH, cm	Canopy Height, m	Median age, years
Upland Pine	2537	22.1 *(8.4)*	691 *(456)*	184 *(75.0)*	0.38 *(0.15)*	22.2 *(5.3)*	14.2 *(2.8)*	75 *(26)*
Lowland Pine	890	24.4 *(11.9)*	873 *(595)*	209 *(102)*	0.42 *(0.21)*	20.9 *(6.1)*	13.5 *(3.5)*	70 *(27)*
Atlantic White Cedar	247	54.0 *(29.0)*	1295 *(959)*	398 *(231)*	0.52 *(0.30)*	25.9 *(11.1)*	16.5 *(4.6)*	91 *(30)*
Swamp Hardwood	205	20.7 *(9.9)*	581 *(427)*	163 *(80.0)*	0.38 *(0.18)*	24.4 *(8.8)*	15.0 *(3.5)*	83 *(32)*
Upland Oak	173	17.5 *(5.9)*	513 *(345)*	143 *(49.6)*	0.38 *(0.13)*	23.0 *(6.1)*	15.4 *(2.9)*	84 *(24)*

these constituted 51% of the 30-min timesteps in the tower data over our study period.

We therefore compared the model's ability to partition fluxes at the 24-hr timestep using daily average values on Landsat image dates that had flux observations with short to no gaps and met methodological assumptions of the eddy covariance technique. We also compared the model's performance against two measures of ET from the flux tower. In addition to the latent energy measurements from the eddy covariance method, we also calculated latent energy as the residual of the energy budget, using Eq. (1):

$$LE = R_n - H - G \quad (1)$$

We converted both of these LE values to ET, designating the direct measurements ET_{direct} and the residual method ET_{closed}. To place the model's performance in context against the inherent variability of the eddy covariance measurements, we compared ET_{closed} and ET_{direct}. We also estimated energy storage terms for the flux tower data to determine if energy storage was meaningful in calculating ET_{closed}, but its effect was small at the 24-hr timestep (approximately 2% of the magnitude of LE in equation 1); for this reason and because the calculation was subject to several assumptions, we ignored energy storage for these analyses. DisALEXI results and queries were processed in R using the packages 'raster'(Hijmans, 2022), 'rgdal' (Bivand et al., 2022), and 'sp' (Pebesma and Bivand, 2005).

2.3. Forest inventory data

Forest inventory data were collected from 2017-2019 in Wharton and Penn State Forests as part of New Jersey Forest Service's process for developing forest management stewardship plans. This dataset contained 6000 plot clusters, each with nested plot measurements to assess the plant community at different scales and resolutions: (a) a variable-radius overstory plot, (b) a 81.3 m^2 ($1/50^{th}$ acre) fixed area advanced-regeneration plot, and (c) a 8.1 m^2 ($1/500^{th}$ acre) fixed area ground-cover plot. The inventory plots were distributed among forest types identified by NJFS through 'heads up' digitization, where the number of plots were allocated among different forest types to achieve smaller sampling error in basal area estimates.

Plot clusters were allocated amongst the forest types to minimize type-level variance in basal area per acre as predicted from an overstory pre-cruise conducted in the same area. For overstory plots in the Atlantic white cedar type, the contractor used a basal area factor (BAF) – 30 (ft^2 $acre^{-1}$, equivalent to 6.9 m^2 ha^{-1}), but for all other overstory plots the contractor used BAF-10 (ft^2 $acre^{-1}$, equivalent to 2.3 m^2 ha^{-1}). This was done to maintain the scale of plot-level sample variance, as Atlantic white cedar stands in the New Jersey Pinelands typically achieve basal areas that are more than triple the basal areas of adjacent uplands.

Plot clusters were considered 'pure' when 80% of the total live basal area for the plot cluster was occupied by the proportions of the species in the type (Appendix A: Table A1). For example, a plot cluster would be labeled 'pure pine' if the sum of the basal area of pitch pine, shortleaf pine, Virginia pine, and/or loblolly pine was equal to or greater than 80% of the total living basal area for all species on the plot. For the purposes of these analyses, we excluded white pine (*Pinus strobus* L.) in relative basal area of pines, as we were more interested in the behavior of more abundant hard pines.

A summary of forest type attributes can be found in Table 1. Overstory summary data included basal area per hectare (m^2 ha^{-1}), trees per hectare, quadratic mean diameter (QMD), and Stand Density Index (SDI). Forest attributes were similar across vegetation types, other than for Atlantic white cedar. Relative density (current Stand Density Index / maximum theoretical Stand Density Index) was calculated using the methods in Dixon and Keyser (2019).

2.4. Land use 2015 dataset

We used the New Jersey Department of Environmental Protection's (NJDEP) Land Use/Land Cover of New Jersey 2015 (LULC15) dataset (New Jersey Department of Environmental Protection, 2019) to sample then later stratify the DisALEXI model outputs. This dataset is the latest in a series commissioned by NJDEP's Bureau of Geographic Information Systems to represent the landscape of New Jersey. The LULC15 data uses a modified hierarchical Anderson Land Use code to designate different cover types, with general cover designations for forest. Classes and their extent can be found in Appendix A: Table A2.

2.5. Forest management & other disturbances

Forest management history was reconstructed from NJFS activity records, aerial images, field reconnaissance, and consultation with private-lands foresters. We digitized polygons around each management activity using contemporaneous aerial imagery; prior to the 1990s there was approximately one set of images per decade, with at least two sets each decade since. We matched the paper records with the appearances of the sites in aerial images to determine the type of forest management that occurred for each polygon, although for many activities, the evidence of prior management can be observed today through current stand structure. For instance, seed trees left from old cuts can today be found amidst their own offspring, made obvious by their drastically different crown architecture, height, and girth. Though there was significant diversity in the intent and execution of silvicultural prescriptions applied, some treatments were more common than others. Most regeneration treatments were seed tree harvests, and most intermediate treatments designed to increase accrual (not ingrowth) were considered to represent applications of thinning rather than other management techniques (like selection harvests). Clearcuts (meant to regenerate a new stand), clearings (intentional and permanent conversion to a non-forest land cover type), selective harvests, and shelterwood cuts were also recorded, though there were too few of these or they occurred too far in the past to make inferences about ET recovery patterns immediately following management. Since 1958 there have been 89 seed-tree harvests and 55 thinning events for which we had records in the study area. After removing pixels for which there had been multiple types of closely-timed disturbance events, we had sufficient data for analysis of 81 seed tree harvests and 53 thinning events, yielding 13,725 and 11,475 pixels respectively.

Records of prescribed burns and wildfires were obtained from the New Jersey Forest Fire Service for the years 2015-2017. For prescribed

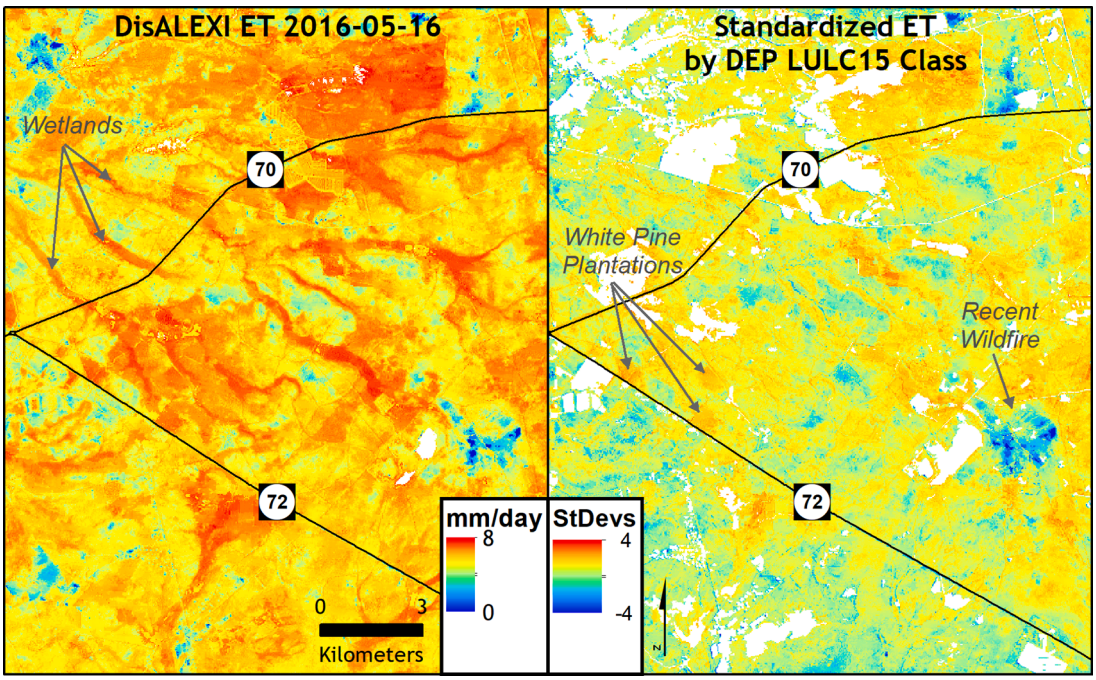


Fig. 2. DisALEXI daily 30m Landsat-like ET (left) on May 16, 2016, and the same image standardized by class means/standard deviations from NJDEP LULC2015 classes (right). Non-forest is masked from the standardized ET on right and appears white. Wetlands are prominent features on the left, highlighting their elevated water consumption at this time of year. Upland pine forests with large components of planted white pines are distinct from wetlands in the standardized image, on right, adjacent to the north side of NJ Route 72.

burning records prior to 2015, we located & digitized burns using a combination of Landsat imagery, aerial imagery, LiDAR, and available paper records. LiDAR-derived ground surface elevation data were useful to locate plow lines, used in this region to assist in the deployment and control of prescribed fire. Their presence indicates an area has been or will be burned. All burn prescriptions in southern New Jersey occurred between November 1 and March 31, during the dormant season for deciduous species. We recorded 616 instances of prescribed burning in the study area from 2001 through 2014, along with 166 areas provided by the NJFFS for 2015-2017. After removing pixels for which there had been multiple types of disturbance events, we were left with 63,572 pixels for analysis across 113 different events (for 2015-2017) to characterize prescribed burning.

Other disturbances were used to screen for overlapping disturbance events. These included wildfires, spongy moth (*Lymantria dispar)* defoliation, and southern pine beetle (*Dendroctonus frontalis)* associated tree mortality. Wildfire data were obtained from the New Jersey Forest Fire Service, while the insect pest data were extracted from USDA Forest Service - Forest Health and Monitoring program data (USDA Forest Service, 2018).

2.6. Analyses

We filtered out pixels that had experienced additional recent disturbances so that overlapping events would not introduce additional variation in our simulations. Pixels that had in the prior 15 years experienced other management activities or a wildfire were excluded, as were pixels that had in the preceding five years experienced a prescribed fire, damage caused by spongy moth or southern pine beetle. Using the included data, we performed three sets of analyses:

1) Comparison of ET for Upland Forest Types from DEP Land Use 2015
2) Comparison of ET for five major forest types of NJ Pinelands from Inventory Data
3) Development of functions to describe the effect of thinning, seed tree harvests, and prescribed burns on ET

These analyses were conducted using the following R packages: 'propagate' (Spiess, 2018), 'pracma' (Borchers, 2022), 'nlstools' (Baty et al., 2015), 'lme4' (Bates et al., 2015), and 'minpack.lm' (Elzhov et al., 2022).

2.6.1. ET and forest inventory points

We used forest inventory data collected for the New Jersey Forest Service to examine ET in the five major forest types of the NJ Pinelands. There were three dominant wetland types in these data (Atlantic white cedar forest, swamp hardwoods, and pine lowland) along with a pair of major upland forest types (upland pine and upland oak).

For each of the compositionally homogeneous inventory plots, we calculated summary statistics. Upland and lowland pine were separated using the LULC15 data. From these groups and across four years of data, we fit a hierarchical mixed effects model to predict annual ET as a function of composition. We compared the AIC (Akaike Information Criterion), BIC (Bayesian Information Criterion), and residual variance of increasingly more complex potential models to select the most appropriate model to describe ET as a function of composition. Candidate models were as follows:

$$ET_{annual} \sim 1 \quad \text{(A1)}$$

$$ET_{annual} \sim ForestType \quad \text{(A2)}$$

$$ET_{annual} \sim ForestType + (1|year) \quad \text{(A3)}$$

$$ET_{annual} \sim ForestType + (1|year) + (1|point) \quad \text{(A4)}$$

where ET_{annual} represents the total annual ET for a point (mm), *ForestType* represents the state inventory-determined major forest type, *(1|year)* represents the random effect variation from the year of observation, and *(1|point)* represents a random effect for each forest inventory point.

2.6.2. ET and DEP LULC15

We selected upland forest types from the LULC15 dataset to examine

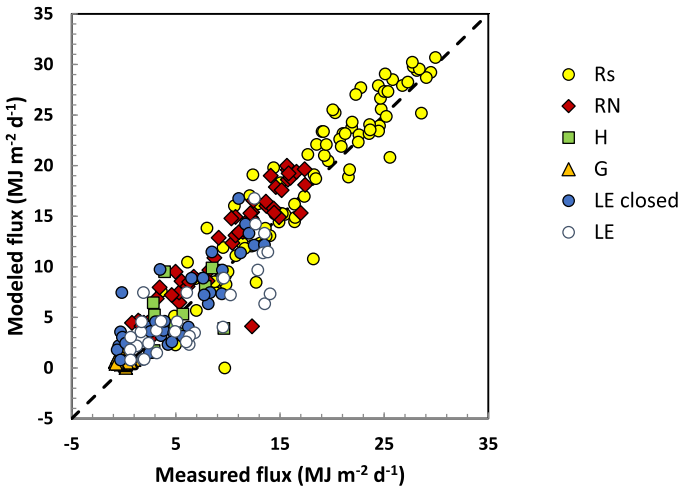


Fig. 3. Energy budget scatter for 24-hour observations on Landsat image dates, 2015-2017. X axis represents observations from US-Slt flux tower, y-axis represents DisALEXI modeled fluxes for the pixel covering the tower. Rs – incoming solar radiation; RN – net radiation; H – sensible heat; G – soil heat flux; LE closed – LE as the residual of Rn-G-H; LE – latent energy flux direct measurement.

the effects of forest composition and canopy cover on ET. There were four composition types in the dataset: Coniferous, Mixed (Coniferous dominated), Mixed (Deciduous dominated), and Deciduous. We further subdivided these categories into two canopy cover groupings (either 10-50% canopy or >50% canopy). We evaluated a range of increasingly complex mixed-effect candidate models for the composition types and canopy cover on annual ET. As with the model selection process for the forest inventory points, we compared the AIC, BIC, and residual variance of potential models to select the most appropriate model to describe ET as a function of the land cover type. Candidate models were as follows:

$$ET_{annual} \sim 1 \quad \text{(B1)}$$

$$ET_{annual} \sim ForestType \quad \text{(B2)}$$

$$ET_{annual} \sim ForestType + CanopyCover \quad \text{(B3)}$$

$$ET_{annual} \sim ForestType + CanopyCover + (1|year) \quad \text{(B4)}$$

$$ET_{annual} \sim ForestType + CanopyCover + (1|year) + (1|pixel) \quad \text{(B5)}$$

$$ET_{annual} \sim ForestType * CanopyCover + (1|year) + (1|pixel) \quad \text{(B6)}$$

where ET_{annual} represents total annual evapotranspiration of a specific pixel in units of mm = year^{-1}, *Forest Type* represents the first three digits of the land use code of the NJDEP Land Use 2015 data, *CanopyCover* represents the fourth digit (level of canopy cover), *(1|year)* represents a random effect for the year of the observation, and *(1|pixel)* represents a random effect for each pixel.

For this analysis, only pixels within Wharton State Forest and Brendan T. Byrne State Forest were examined. The deciduous upland forest types on these properties are mainly oak-dominated with an ericaceous understory, making them distinct from the otherwise mixed-species deciduous upland forests elsewhere in the inner coastal plain. This reduced the variance in the classes described in the land-use data so that we could make Pinelands-specific comparisons.

2.6.3. ET as a function of management

We applied non-linear least squares models at different time steps to determine the response of forest ET to different types of management, restricted to those activities that were frequent enough in the study area to have sufficient data for modeling: seed-tree harvests, thinning, and prescribed burning. We used a model of the form in (2) to describe the ET response to management:

$$ET_{std}(t) = \left(\frac{\beta_1}{1 + \exp(\beta_2 * (t - \beta_3))}\right) - 10 \quad (2)$$

where ET_{std} *(t)* is a standardized representation of the pixel's evapotranspiration (described below) at the timestep *t*, β_1 represents the maximum value of post-disturbance ET_{std}, β_2 represents the slope of the recovery of ET_{std} post-disturbance, and β_3 represents the inflection point or time of most rapid recovery in ET_{std}. The offset value (10) was used to ensure that sign did not affect model behavior when crossing zero.

To account for differences in the magnitude of the water budget between years, as well as differences in ET between forest types, we performed a stratified standardization of pixel ET values (Fig. 2), where strata were the cover types from LULC15 dataset. For this we standardized against pixels over Wharton and Brendan T. Byrne State Forests to ensure that the cover types corresponded to consistent physical forest types. For each timestep *t* we computed class-wise means and standard deviations in ET. A standardized anomaly in ET (ET_{std}) was then computed for each pixel at that timestep, representing the divergence in standard deviations from the mean value for that pixel's forest type.

Different disturbance types were evaluated at different timesteps. For thinning and seed tree harvests, we compared standardized annual ET to time since disturbance, while for prescribed fire we evaluated standardized daily, weekly, monthly, and annual ET. For prescribed fire data at the daily, weekly, and monthly analysis scales, there were sufficient standardized data to ignore missing values. Due to the longer timespan of annual summaries, the small amount of missing pixel values from DisALEXI (<2% of growing season observations, ~6% of dormant season observations) required filling so as not to exclude an observation with only 364 daily values. For annual summaries only, we filled missing daily pixel values with the corresponding month's average daily ET for that pixel; from this time-series we calculated annual ET and ET_{std}.

We used repeated subsampling of each management activity's dataset to establish a distribution of model terms. For each type of activity, we pooled the data from all 4 years, drew a random 50% subsample, fit the Eq. (2), and repeated the process 10,000 times.

To determine the duration of the effects on ET, we used the model simulations to mark the point in time at which only 5% of the post-disturbance anomaly remained. From time = 0 (time of disturbance) to the 5% mark, we calculated the integral of the model to determine the amount of water yielded by the management activity (in standard deviations, see standardization procedure above). When the model's maximum value (β_1) was less than 0, we calculated the integral below the maximum value, rather than to zero.

3. Results

3.1. Comparison of DisALEXI and eddy flux data

In comparison with flux observations from US-Slt, DisALEXI provided reasonable partitioning of the surface energy budget on Landsat overpass dates (Fig. 3). Employing the data fusion strategy to estimate time-continuous daily ET, DisALEXI was also able to characterize seasonal and daily variability in flux observations over the four-year study period (Fig. 4).

Quantitative comparison with flux measurements yielded good agreement between DisALEXI and both closed and unclosed methods of ET tower-based observation (Fig. 5a, Table 2). Residual closure tended to lower daily ET by approximately 25% (Fig. 5b) and provided better agreement with modeled fluxes, reducing RMSD (MAE) from 1.25 (0.91) to 1.08 (0.81) mm d^{-1} at the daily timestep, consistent with results from prior studies in forested systems (Yang et al., 2021a). Agreement at peak flux, however, was better without closure corrections to observed fluxes. Model errors decrease at weekly timesteps due to cancellation of random

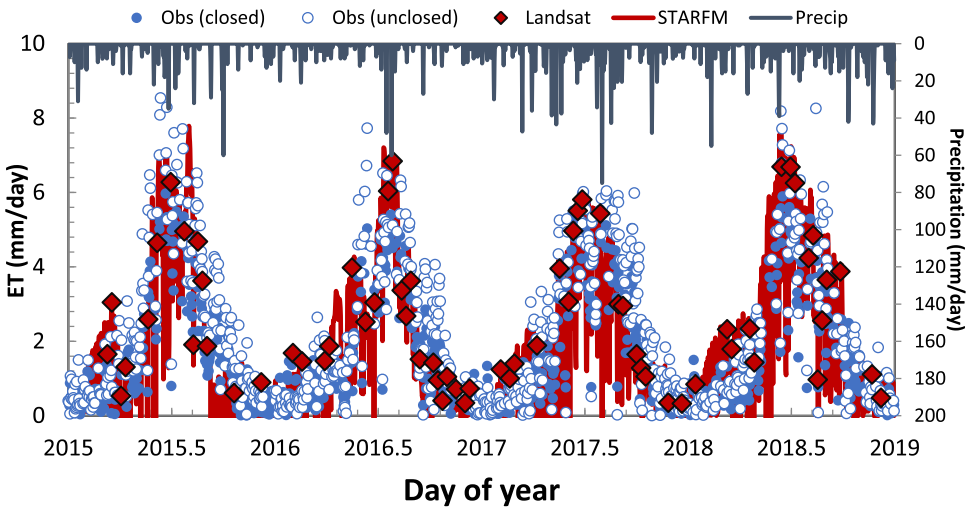


Fig. 4. Comparison of DisALEXI model performance against US-Slt flux tower data. Hollow circles represent 24-hour sums of ET from direct flux measurements of LE; solid circles represent 24-hour sums of ET based on the residual of Rn-G-H. Diamonds represent observations of ET derived from the DisALEXI model downscaled using Landsat imagery; lower lines represent ET determined at Landsat-scale by the STARFM algorithm for all other dates. Precipitation depth is reversed from the top edge of the plot and shown on the right-hand y axis.

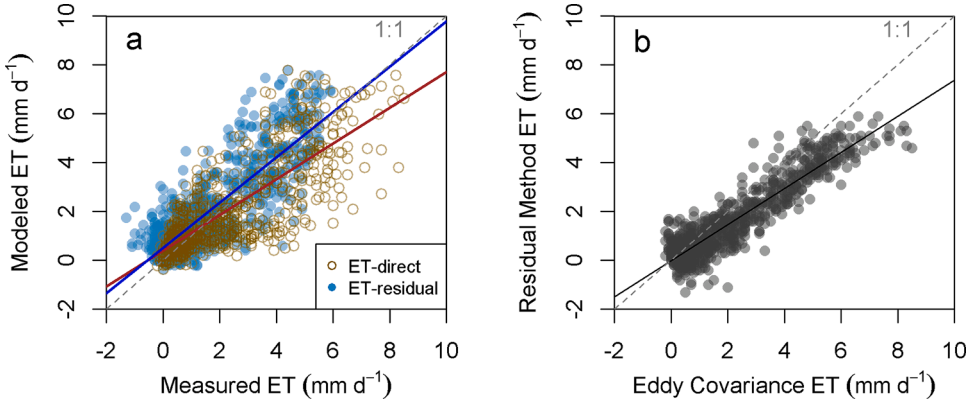


Fig. 5. Comparison of ET between DisALEXI model, direct eddy covariance measurements, and the residual of the energy budget. ET-residual is equivalent to Rn-G-H. (a) shows the relationship between modeled ET and both tower-based methods, with a best fit line for each. Upper line (blue) shows regression of ET-residual as a function of DisALEXI, lower line (brown) shows regression of ET-direct observation as a function of DisALEXI. (b) shows the variation between both methods of tower observation, with the solid black line showing the regression of the direct measurement as a function of the residual. (For interpretation of the references to color in this figure legend, the reader is referred to the web version of this article.)

Table 2
Metrics of flux model accuracy. N, number of observations excluding gaps; $\bar{O}$, mean observed flux; MBE, mean bias error; RMSE, root mean square error; MAE, mean absolute error; RE, relative error (MAE/MeanO).

STARFM ET	N	$\bar{O}$	Slope	MBE	RMSE	MAE	R^2
Daily (closed)	767	1.81	0.99	0.32	1.08	0.81	0.69
Daily (unclosed)	769	2.25	0.73	−0.21	1.25	0.91	0.62
Weekly (closed)	66	1.83	1.10	0.30	0.88	0.65	0.77
Weekly (unclosed)	69	2.12	0.81	−0.24	0.99	0.70	0.69

errors to 0.88 (0.65) mm d^{-1} with residual closure.

3.2. ET and forest inventory types from inventory points

The mixed effects model A4 produced estimates for the variation in total annual ET in mm = $year^{-1}$ introduced from annual differences (1|*year* term, random effect), variation between plots (1|*plot* term, random effect), and the fixed effects of the different forest types (*ForestType* term) (Table 3). Model A4 had by far the lowest AIC, BIC, and residual variance of any of the models evaluated and was a significant improvement upon the null (A1) and less complex nested models (models A2 & A3).

We found clear differences between most of the major Pinelands forest types in each of the study years (Fig. 6, Table 4). Relative ET differences among groups were consistent between years. Oak uplands

Table 3
Likelihood ratio test for candidate models to predict annual ET by inventory-derived cover type. Significance of *** indicates model significance at <0.001.

Likelihood ratio test
Model A1: $ET_{annual} \sim 1$
Model A2: $ET_{annual} \sim$ ForestType
Model A3: $ET_{annual} \sim$ ForestType + (1|year)
Model A4: $ET_{annual} \sim$ ForestType + (1|year) + (1|point)

Model	npar	Log Likelihood	X^2	Pr(>X^2)	Significance	AIC	BIC	Residual variance
A1	2	-79380	0			158764	158779	12283
A2	6	-77858	3043.5	<2.2e-16	***	155728	155773	9714
A3	7	-76929	1858.9	<2.2e-16	***	153872	153924	8397
A4	8	-73261	7336.4	<2.2e-16	***	146537	146597	2728

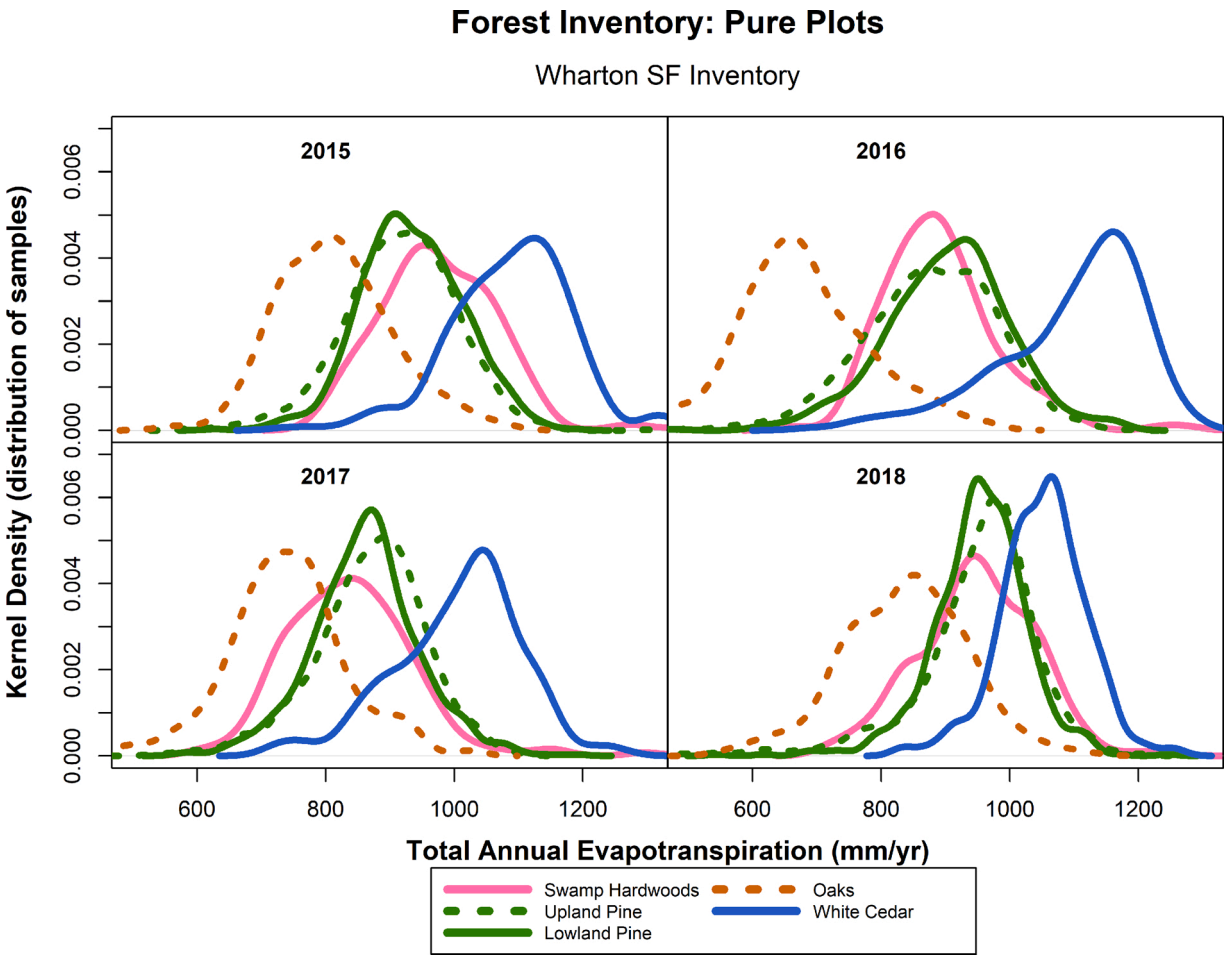


Fig. 6. Distributions of annual ET, 2015-2018, for five different forest types identified through the New Jersey Forest Service inventory data of Wharton and Penn State Forests.

Table 4
Mixed effects model results examining ET as a function of forest types identified in Wharton State Forest Inventory data, 2017-2019.

Forest type	Sample size (*n* plots)	Predicted ET_{annual} (mm $year^{-1}$) MLE	Confidence intervals for predictions			
			2.5% Random & fixed effects	Fixed -effects only	97.5% Fixed -effects only	Random & fixed effects
Atlantic White Cedar	236	1060.6	886.4	1018.3	1102.9	1234.7
Swamp Hardwoods	184	914.4	740.1	871.7	957.0	1088.6
Lowland Pine	730	915.2	741.2	873.7	956.6	1089.1
Upland Pine	1945	903.7	862.5	903.7	944.9	1077.6
Oak	144	768.2	593.9	725.2	811.3	942.6

Fixed effects	Est.	Std. error	t value	Random effects	Variance	SD	+/- 1.96 SD (mm $year^{-1}$)
Atlantic white cedar	1060.6	21.6	49.2	Year	1755	41.9	82.1
Swamp Hardwoods	−146.2	7.8	−18.6	Plot (between plot)	5676	75.3	147.7
Oak	−292.3	8.4	−34.7	Residual (within plot)	2728	52.2	102.3
Lowland Pine	−145.4	6.0	−24.4				
Upland Pine	−156.9	5.5	−28.5				

had the lowest annual ET (mean = 768 mm $year^{-1}$), Atlantic white cedar had the highest annual ET (mean = 1060 mm $year^{-1}$), and pine types had intermediate ET (mean = 915 mm $year^{-1}$ and mean = 903 mm $year^{-1}$ for lowlands and uplands, respectively). Swamp hardwoods were both intermediate (mean = 914 mm $year^{-1}$) and variable, and their place in the order of ET varied by year.

Of the random effects, variance between plots was greater than that between years. Separate from the effect of the year, the model residual variance (within-plot variance between observations at the same location) was greater than the effect of the year, but less than the variance between plots. The between-plot (Plot) term incorporates variation in forest structure between plots such as varying levels of leaf area index (LAI), disparities in occupancy of growing-space, different understory characteristics, changing groundcover, variation in mean canopy height, and any number of other forest attributes that vary among inventory plots, any combination of which might impact ET.

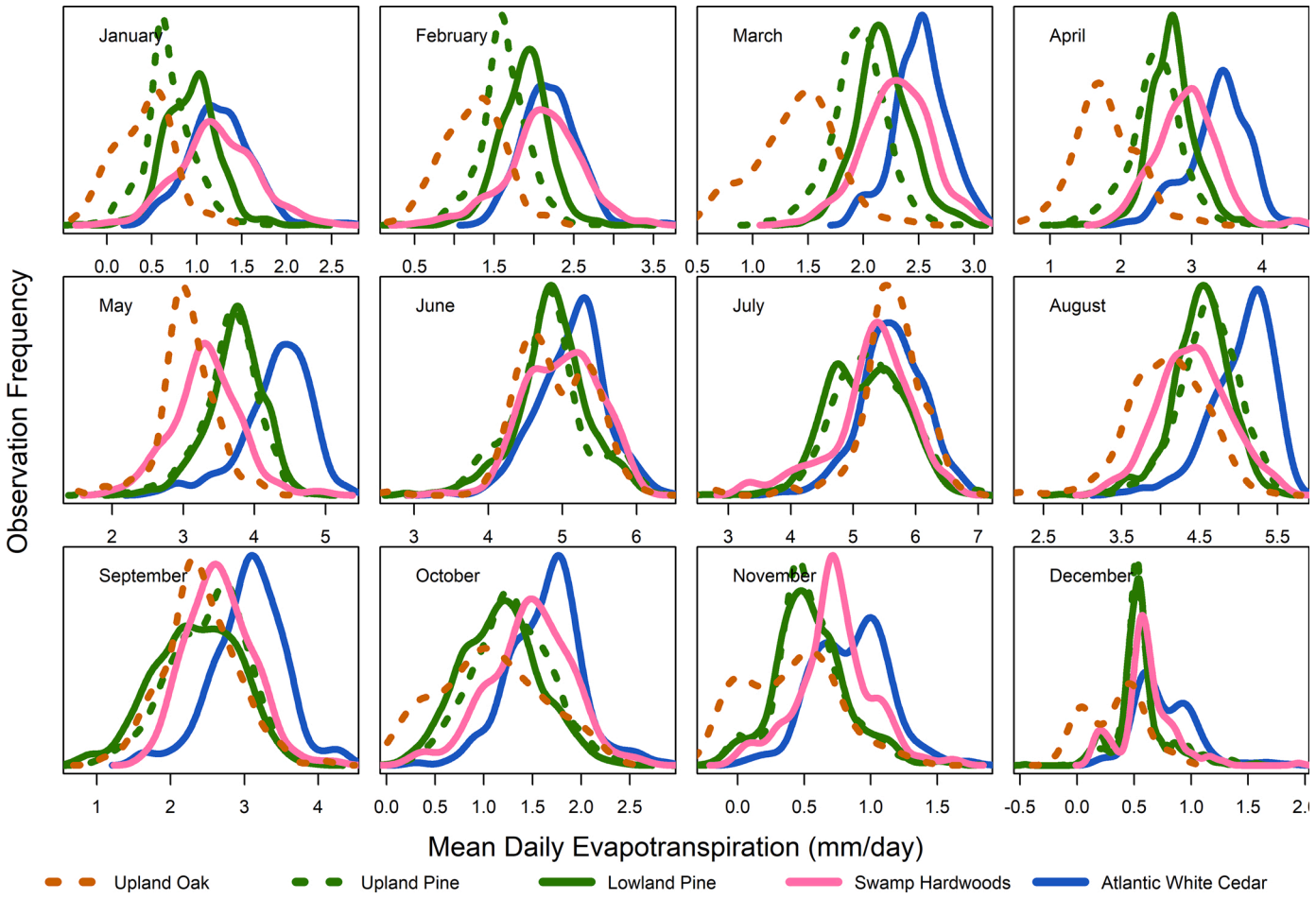


Fig. 7. Distributions of daily average ET by month, 2015. Forest type data from NJFS inventory of Wharton State Forest. Delay in leaf-out until May coincides with the lower ET rates for oak-dominated plots versus pine.

We found temporal differences in ET that corresponded to the phenology of the dominant species in the inventory plots (Fig. 7). For all years, oak-dominated plots had lower average daily ET rates in March, April, and May. In most months, cedar plots had high ET rates, but during spring and autumn the increased ET rate of cedar was more pronounced. The only year for which cedar did not have higher ET rates in the fall was 2018, which was the wettest year on record in the study area.

3.3. ET and DEP LULC15

Comparison of the distributions of ET among the NJDEP Land Use 2015 upland forest types (Fig. 8) showed meaningful differences related to forest composition and canopy cover. ET increased with increasing proportion of conifers, in both closed-canopy polygons (> 50% canopy cover) and open-canopy polygons (10-50% canopy cover).

Model B6 was a significant improvement upon the null (B1) and nested less-complex models (B2, B3, B4), and produced a lower AIC and BIC than model B5 (Table 5). Model effects and estimates for B6 can be found in Table 6.

Closed-canopy coniferous upland forest (solid green lines in Fig. 8) used approximately 164 mm more water per year (17%-18%) than closed-canopy deciduous upland forest (solid brown lines). Higher canopy cover (the solid lines) also corresponded with higher ET for the coniferous forest type: we observed an increase of approximately 61 mm year^{-1} for coniferous forest labeled as having >50% canopy cover over the 10-50% canopy cover class of conifer stands, and a 33 mm year^{-1} increase in ET for the >50% canopy cover mixed coniferous-dominated class. We observed the opposite effect in the deciduous forest types: >50% canopy cover was associated with 15 mm year^{-1} lower ET for the mixed deciduous-dominated class, and 31 mm year^{-1} lower ET for the deciduous classes. The effect of increased canopy cover on annual ET was directly proportional to increasing dominance of coniferous trees: as the forest became more dominated by conifers, higher canopy cover was associated with ever-higher ET. Within-pixel variance (model residual) was about the same magnitude as the effect of the year, but much less than variance between pixels (pixel term).

3.4. ET as a function of management

3.4.1. Effect of thinning

Thinning affected forest ET in the years immediately following cutting. By approximately 5-10 years post-activity, thinning had little discernable impact on ET_{std} (Fig. 9; Fig. 10). After 5.9 years (5.67-6.20 years, 95% credible interval from simulation approach), the anomaly in ET_{std} had diminished to 5% of the original maximum effect size post-cutting (Table 7). In the time between cutting and when the model reached 5% effect level, the time-integrated difference in ET_{std} between an unthinned and thinned pixel showed a net accumulated effect of thinning of -4.1 annual standard deviations (95% credible interval from -4.0 to -4.3), accounting for the offset of the model's maximum value. Standard deviations here correspond to the standard deviation in the distribution of ET for pixels falling in the same NJDEP cover type for any given year. For example, the annual standard deviation of ET for pixels in the predominant NJDEP forest cover type, coniferous forest with >50% canopy cover, was 88 mm, 98 mm, 83 mm, and 90 mm for 2015 to

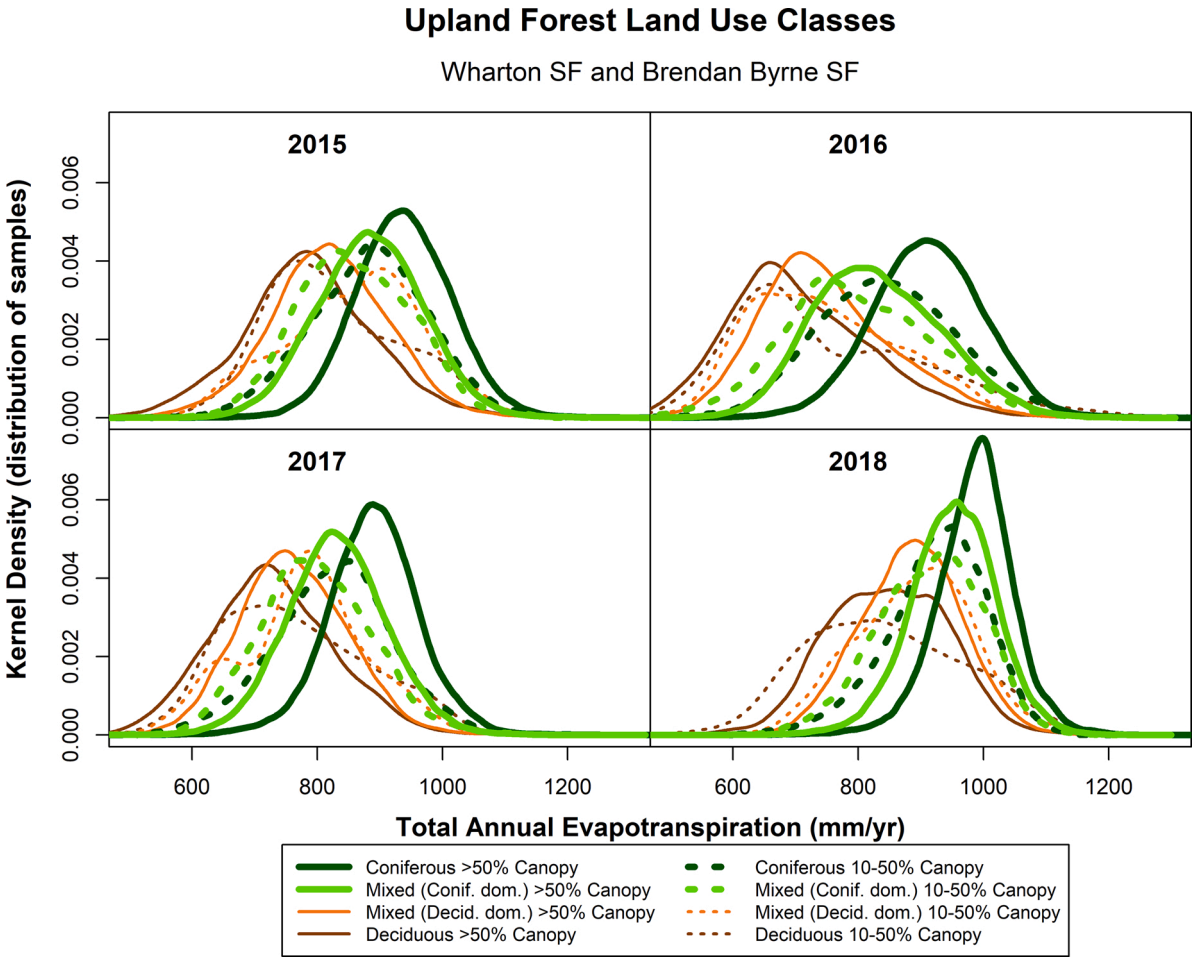


Fig. 8. Distributions of annual evapotranspiration for 2015-2018 for four forest compositions and two levels of canopy cover, as identified by the New Jersey Department of Environmental Protection Land Use/Land Cover 2015 dataset.

Table 5
Likelihood ratio test for candidate models to predict annual ET by selected Land Cover 2015 codes. Significance of *** indicates model significance at <0.001.

Likelihood ratio test
Model B1: $ET_{annual} \sim 1$
Model B2: $ET_{annual} \sim$ ForestType
Model B3: $ET_{annual} \sim$ ForestType + CanopyCover
Model B4: $ET_{annual} \sim$ ForestType + CanopyCover + (1|year)
Model B5: $ET_{annual} \sim$ ForestType + CanopyCover + (1|year) + (1|pixel)
Model B6: $ET_{annual} \sim$ ForestType * CanopyCover + (1|year) + (1|pixel)

Model	npar	Log Likelihood	X^2	Pr(>X^2)	Significance	AIC	BIC	Residual variance
B1	2	−6296374				12592753	12592776	11928
B2	5	−6169149	254451	< 2.2e-16	***	12338307	12338367	9318
B3	6	−6154944	28409	< 2.2e-16	***	12309900	12309971	9064
B4	7	−6042255	225378	< 2.2e-16	***	12084524	12084607	7283
B5	8	−5766751	551008	< 2.2e-16	***	11533519	11533614	2481
B6	11	−5765773	1956	< 2.2e-16	***	11531568	11531699	2481

2018, respectively.

3.4.2. *Effect of Seed tree harvest*

Seed tree harvests depressed ET to a greater extent and for a longer duration than did thinning (Figs. 11, and 12). Model term B_2 (slope of recovery) was smaller following seed tree harvests than it was for thinning, highlighting the slower pace of recovery (Table 8). Further, ET_{std} immediately after treatment was lower for seed tree harvests than thinning, reduced by twice as many standard deviations by the seed tree harvest. To recover to the same 5% of effect size for a seed tree harvest took 12.8 years (12.6-13.0 years, 95% credible interval from simulation approach). In the time between treatment and when the model reached 5% effect level, the time-integrated difference in ET_{std} between an uncut and a seed-tree harvested pixel showed a net accumulated effect of -28.7 annual standard deviations (95% credible interval from -28 to -29).

3.4.3. *Effect of prescribed fire*

Direct impacts to ET due to prescribed fire were variable. We were unable to fit a recovery function of the same form as Eq. (2) to the prescribed burn data, but a visual evaluation of the data showed an average effect lasting approximately 22 weeks (Fig. 13). Most burns occurred in February and March, meaning that forest ET returned to

Table 6
Mixed effects model results examining ET as a function of NJDEP Land Use/Land Cover 2015 categories.

Upland forest type	Canopy cover	Sample size (*n* pixels)	Predicted ET_{annual} (mm $year^{-1}$) MLE	Confidence intervals for predictions 2.5% Random & fixed effects	2.5% Fixed -effects only	97.5% Fixed -effects only	97.5% Random & fixed effects
Coniferous	10-50%	22,815	869.8	705.9	828.4	911.1	1033.6
Coniferous	>50%	129,792	931.1	772.4	923.6	938.6	1089.8
Mixed-Coniferous	10-50%	2,178	841.7	683.1	840.2	843.2	1000.2
Mixed-Coniferous	>50%	50,736	874.3	715.7	873.1	875.5	1032.8
Mixed-Deciduous	10-50%	1,276	818.6	660.1	815.4	821.9	977.2
Mixed-Deciduous	>50%	34,981	803.2	644.7	801.9	804.5	961.7
Deciduous	10-50%	373	798.1	639.5	793.9	802.3	956.7
Deciduous	>50%	15,379	766.8	608.2	765.4	768.2	925.3

Fixed effects	Estimate	Std. error	t value	Random effects	Variance	SD	+/- 1.96 SD (mm $year^{-1}$)
Coniferous 10-50%	103.0	0.765	134.6	Year	1781	42.2	135.2
Coniferous >50	164.3	0.626	262.6	Pixel	4761	69.0	82.7
Mixed-Conif.10-50	74.9	1.68	44.6	Residual	2481	49.8	97.6
Mixed-Conif.>50	107.5	0.675	159.2				
Mixed-Decid.10-50	51.9	2.14	24.3				
Mixed-Decid.>50	36.4	0.710	51.3				
Deciduous 10-50	31.3	3.84	8.15				
Deciduous >50	766.8	21.1	36.3				

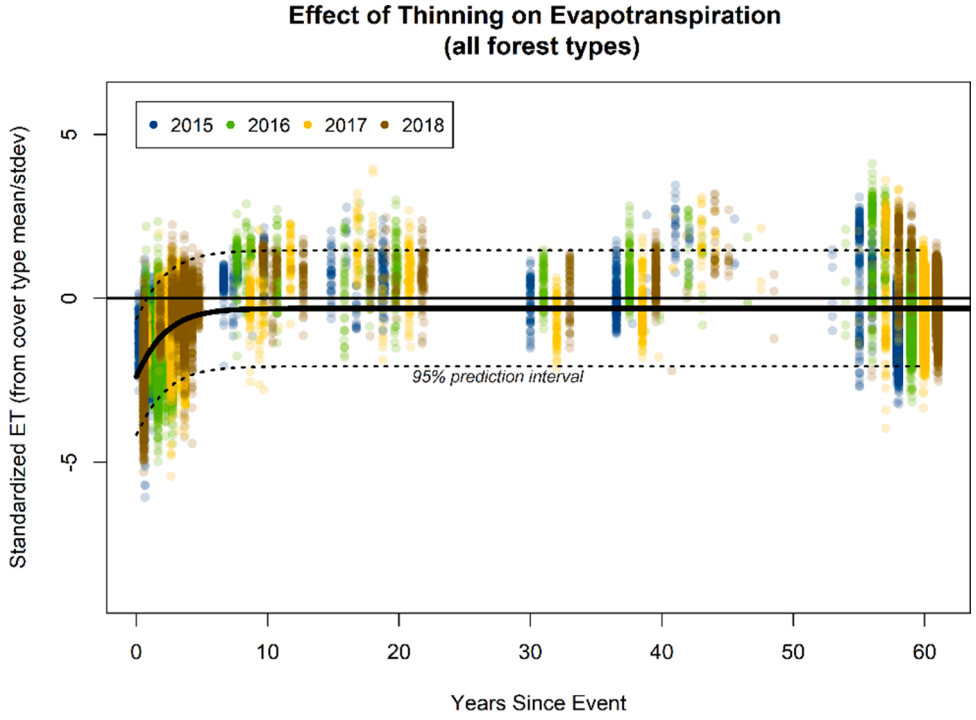


Fig. 9. Effect of thinning on standardized annual ET. Model fit using 2015-2018 data; dotted lines are 95% prediction intervals. Points represent annual ET for a pixel expressed as the number of standard deviations away from the mean annual ET for the corresponding cover type of that pixel.

normal by the beginning of August.

We observed event-specific patterns when each instance of prescribed fire was plotted separately (see Appendix B: Figs. B1, B2 and B3). For some burns there was a modest depression of ET_{std} post-burn, while for others, prescribed fire had no effect or coincided with increased ET_{std}. Even for those fires that were followed by depressed ET_{std}, however, the effect generally did not last longer than a single growing season.

Prescribed fires that demonstrated a decrease in ET for part of the growing season were limited to those higher intensity burns where canopy leaf area was extensively consumed or killed. An example of a set of a range of burn intensities can be seen in Figs. 14 and 15. Burn blocks 'A' and 'B' were burned less intensely than blocks 'C' and 'D'. Flame heights largely did not reach tree crowns in 'A' and 'B'; heat from the flames partially killed but did not consume foliage in 'B'. In contrast, flame heights in blocks 'C' and 'D' consistently exceeded the height of the crown so that nearly all leaf tissue was consumed; this can be seen from the photo in lower left panel of Fig. 14, showing the condition of block 'D' around one month post-burn. Although there was significant overstory mortality in 'D' and some mortality in 'C,' a plot of weekly mean ET_{std} for three years post-burn (Fig. 15) shows that the reduction in

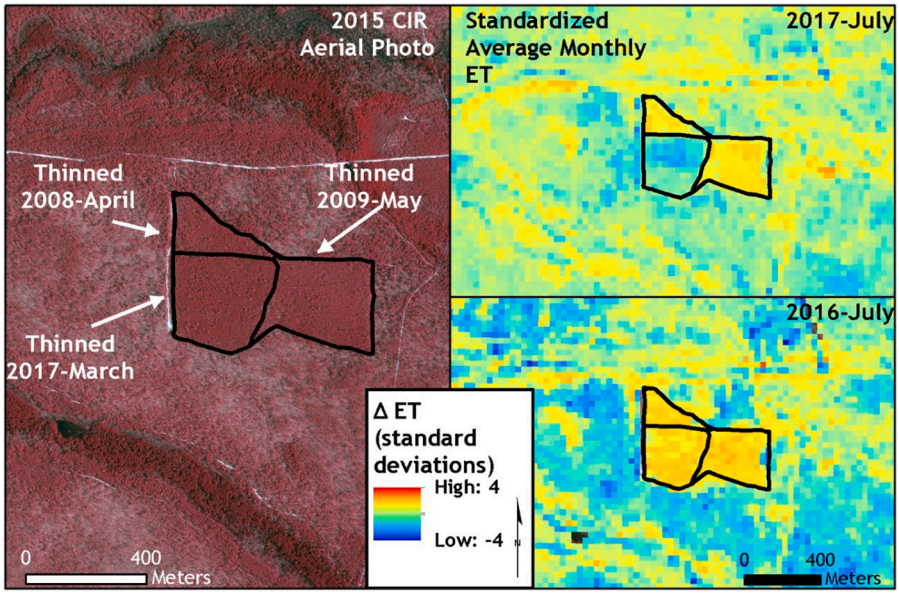


Fig. 10. Example of the duration and intensity of the effect of thinning on forest ET. Change in ET corresponds to the number of standard deviations derived from Land Use 2015 class-wise values for month-by-month averages of average daily ET. For example, a change in ET of -4 standard deviations represents a pixel that, for that month, has an average daily ET that is 4 standard deviations below the monthly average for that land use code. Selected area is in Brendan T. Byrne State Forest, Woodland Township, New Jersey.

Table 7
Simulation results for parameters describing recovery of ET after thinning.

Term	Mean	SD	2.5% quantile	97.5% quantile
β_1 (β_1-10)	−0.301	0.00555	−0.312	−0.290
β_2	−0.544	0.0128	−0.570	−0.520
B_3	−2.38	0.0888	−2. 56	−2.21
Duration of Effect: Years until 5% left to recover	5.94	0.134	5.67	6.20
Integral of Model from t_0 to $t_{5\%}$ (units are σ of annual ET_{std})	−4.12	0.070	−4.26	−3.99

ET from these burns persisted only in cases of the highest burn intensity. The more common applications of prescribed fires were not observed to widely cause a reduction in ET lasting through the growing season immediately after burning (Fig. 13). Block 'D' also occurs in the pitch pine plains, an area of short-stature forest dwarfed by the selective pressure of repeated fires.

4. Discussion

4.1. DisALEXI model performance

Use of the DisALEXI model enabled characterization of both the effects of stand-level management on ET and the impact of plot/stand-

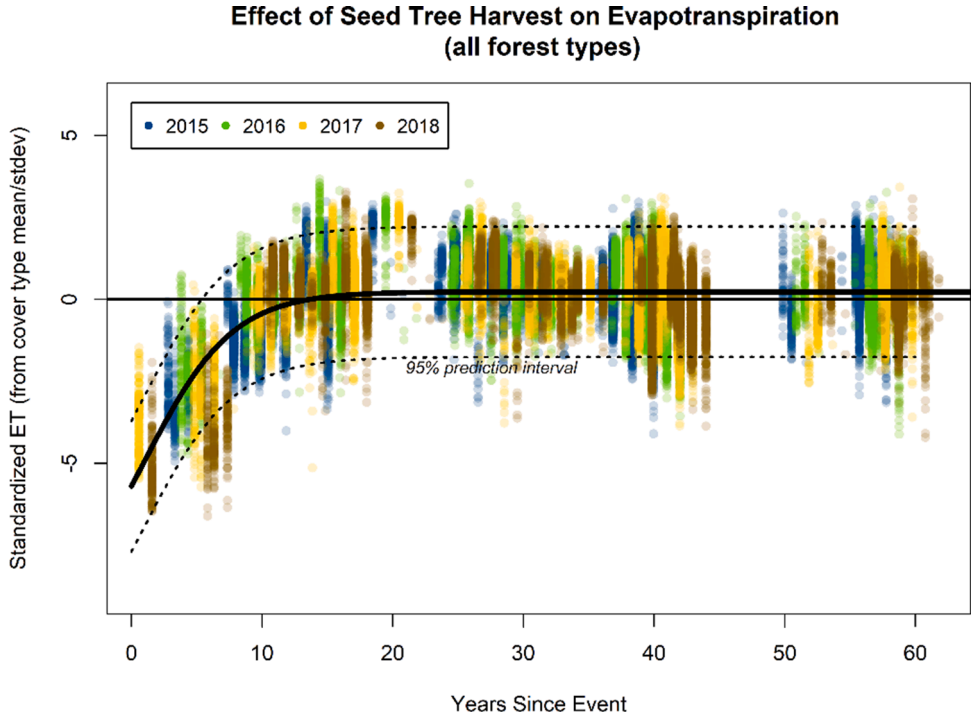


Fig. 11. Effect of seed tree harvesting on standardized annual ET. Model fit using 2015-2018 data; dotted lines are 95% prediction intervals. Points represent annual ET for a pixel expressed as the number of standard deviations away from the mean annual ET for the corresponding cover type of that pixel.

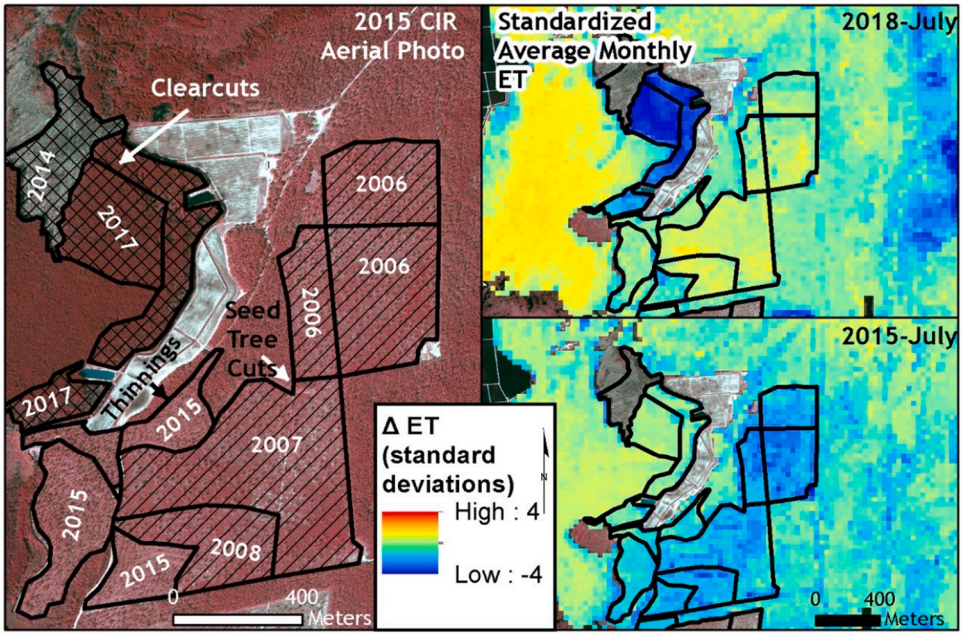


Fig. 12. Effect of seed tree harvests on forest ET. Note that the recovery of ET for thinned areas (open polygons) occurred around the same time as seed tree harvests (diagonal hatching), though the seed tree harvests happened 7-9 years earlier. Private land in Washington Township, Burlington County, New Jersey.

Table 8
Simulation results for parameters describing recovery of ET after seed tree harvest.

Term	Mean	SD	2.5% quantile	97.5% quantile
β_1 (β_1-10)	0.238	0.00559	0.227	0.248
β_2	−0.299	0.00317	−0.305	−0.293
B_3	1.07	0.0760	0.924	1.221
Duration of Effect: Years until 5% left to recover	12.8	0.102	12.6	13.0
Integral of Model from t_0 to $t_{5\%}$ (units are σ of annual ET_{std})	−28.7	0.311	−29.3	−28.1

level forest type & canopy cover on ET. We were able to take advantage of the model's extensive spatial coverage and substitute space for time in evaluating the effects of forest management activities on ET. Functional differences in water use due to forest type could be clearly identified (oak vs. pine upland) which were partially the result of phenological impacts on ET. The fine temporal and spatial scale of the remote sensing data also allowed a more thorough exploration of the effects of prescribed fire on ET, where the variations in fire intensity could be better discerned at daily to weekly rather than annual time scales. These characteristics make DisALEXI especially suitable for examining the interactions of seasonality, disturbances, and forest attributes on forest ET.

The DisALEXI model has been successfully used to characterize the energy budget in agricultural (Anderson et al., 2018; Knipper et al., 2020; Yang et al., 2021a) and forested ecosystems (Yang et al., 2017, 2019, 2021). The errors observed at the US-Slt tower site are comparable to those determined over loblolly pine and mixed forest by Yang et al. (2017, 2019, 2021a), who report RMSE of 1.0-1.6 mm d^{-1} and MAE of 0.8-0.9 mm d^{-1} at daily timesteps. As in prior studies, model estimates agreed better with tower fluxes corrected for energy balance closure (Fig. 4). Sources of disagreement arise from both the model and the tower-based measurement. For example, the size and location of the contributing area to the eddy covariance-measured fluxes varies with windspeed and direction (Burba, 2013). Such variation introduces discrepancies in the comparison with remote sensing-derived values of ET based on the choice of which pixels to include in the comparison; we used only the 9-pixel window around the tower for comparison. Additionally, although eddy-covariance data can produce high-quality measurements of fluxes like ET, they are still subject to limitations. For instance, characterizing annual ET through eddy covariance commonly requires gap-filling for timesteps when atmospheric conditions produce low-quality measurements, when assumptions of the instrumentation are violated, and when instruments fail. Despite a diversity of empirical approaches for gap-filling, these still potentially introduce additional error (Moffat et al., 2007) that may disagree with true values, and with other methodologies. Incomplete flux tower data limited the time periods that we could evaluate DisALEXI model performance while exemplifying the benefits of a remote-sensing model approach.

4.2. *Effects of forest composition on evapotranspiration*

Our modeled ET rates for forests in this region were somewhat higher than observed in other studies. The DisALEXI-based estimates in the cedar forest type and in pitch pine lowlands are higher than eddy-flux annual ET as observed by Sumner et al. (2012) in a mixed pitch pine lowland that contained cedar (cedar, this study: 1060 mm $year^{-1}$; pitch pine lowland, this study: 915 mm $year^{-1}$; mixed lowland, Sumner et al. 2012: 801 mm $year^{-1}$). Schäfer et al. (2014) observed a total annual ET rate of 627 mm $year^{-1}$ for the oak stand at the Silas Little Experimental Forest site flux tower over 2006-2011, though annual ET averaged 664 mm $year^{-1}$ for the non-drought years. Clark et al. (2012) measured ET with the eddy covariance method in the same landscape in 2005-2009, finding lower absolute ET for oak (range:442-699 mm $year^{-1}$), lower absolute ET for pine (593-759 mm $year^{-1}$), and lower ET for mixed upland forest (419-607 mm $year^{-1}$). Those observations occurred during a major infestation of spongy moth which defoliated oaks and understory vegetation during the late spring and summer months, and with prescribed burns applied to the pine and mixed forest sites, all of which exerted downward pressure on annual ET. These are in contrast with our observation for oak stands of 768 mm $year^{-1}$ (95% CI using random and fixed effects 594-943 mm $year^{-1}$) using state forest inventory data, and 767 mm $year^{-1}$ (95% CI using random and fixed effects 608-925 mm $year^{-1}$) for deciduous upland forests with greater than 50% canopy cover using Land Use 2015.

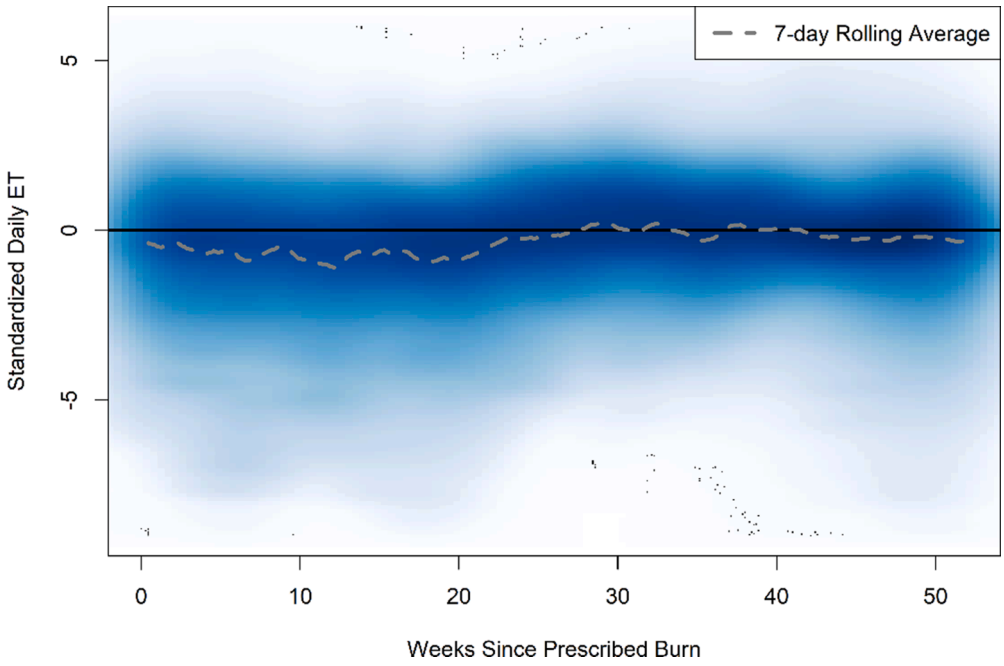


Fig. 13. Effect of prescribed fire on ET. Data shown are for prescribed fires from 2015 through 2017. Broken line represents the 7-day rolling window average standardized ET post-fire, and shading density corresponds to the density of pixel observations.

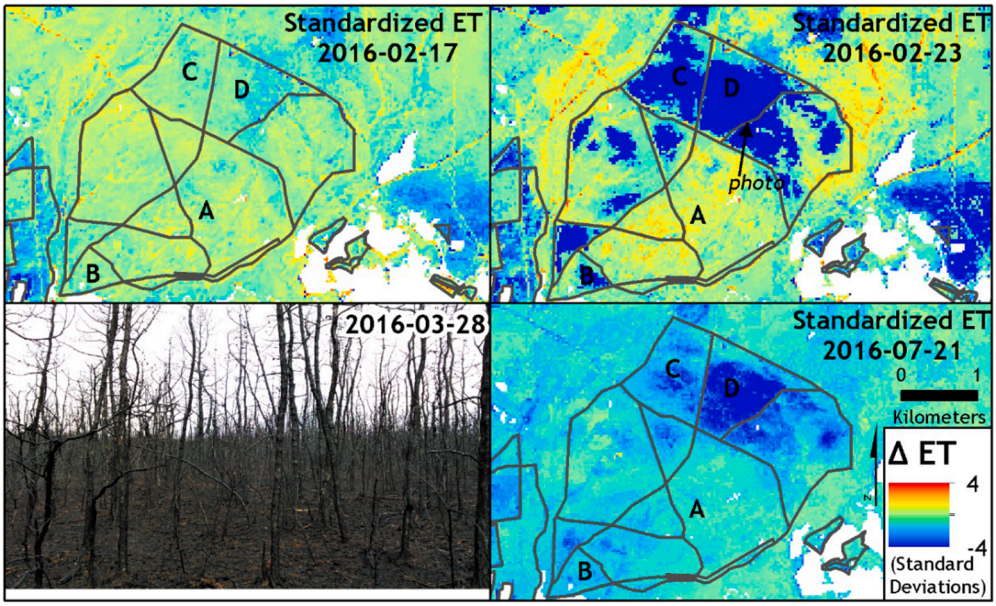


Fig. 14. Spatial example of the varying effects of prescribed fire on ET after disturbance; each gray polygon represents a discrete prescribed burn block. Clockwise from top left: standardized ET pre-fire, standardized ET immediately post-fire, standardized ET approximately 20 weeks post-fire, and a photo of site D post-fire showing the severity of the burn and the edge of the 'pine plains' forest type. Penn State Forest, New Jersey. Photo by the authors.

We observed that increasing proportions of conifers resulted in increased annual ET in uplands (Fig. 8; Table 6). Though the coniferous forests in our area originated largely from natural regeneration, they exhibit the same higher ET compared to deciduous trees as observed in conifer plantations elsewhere (Ford et al., 2011; Komatsu et al., 2008; Swank and Douglass, 1974). It is possible that this contrast between conifer and deciduous upland is a function of stand structural characteristics; oak points in the forest inventory data had the lowest mean basal area (BA) as well as the lowest stand density index (SDI) of the major forest types. Lower BA or SDI has been associated with lower leaf area in other hard pine forest types (Ex and Smith, 2013; McLaughlin et al. 2013). However, the relative density index for oak plots was comparable with that of upland pine, indicating comparable site occupancy for oaks and pines.

Phenology was partially responsible for the ET difference we observed between oak and pine. Oaks are the last tree species to leaf out in the study area, and prior to leaf out in May oak-dominated inventory plots had the lowest ET. Beamesderfer et al. (2020) similarly found that a forest dominated by white pine (*Pinus strobus*) had higher interception losses while a nearby white oak (*Quercus alba*) remained leafless, and that unlike oak the pine trees transpired in the spring and autumn when leaf/soil temperatures were warm enough to support photosynthesis.

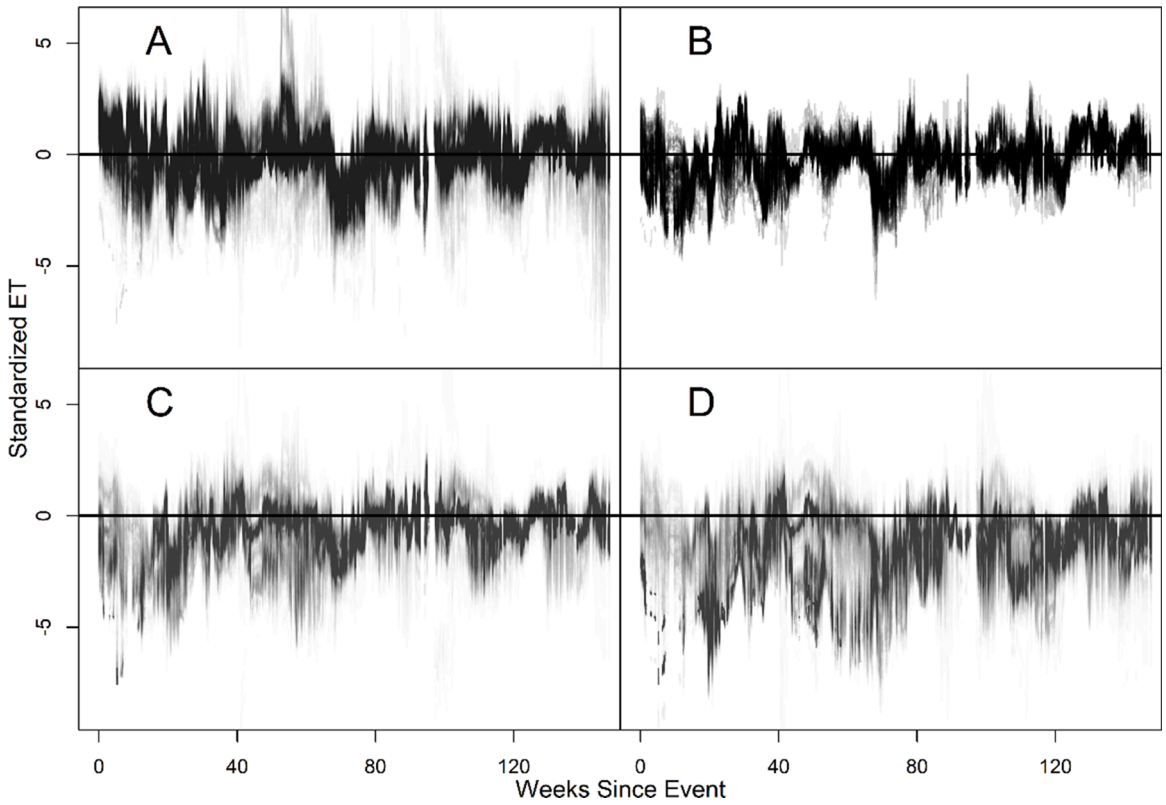


Fig. 15. Example of varying effects of prescribed fire on ET. Each thin grey line is the daily mean standardized ET for a single pixel; darker areas indicate more pixels within the specific burn sharing values for a given week. Letters correspond with polygons in Fig. 14.

Table A1
Overstory tree species in typic forest types.

Forest type	Atlantic white cedar	Swamp hardwood	Pine	Oak	
Species	Atlantic White Cedar (*Chamaecyparis thyoides*)	Red Maple (*Acer rubrum*)	Pitch Pine (*Pinus rigida*)	Black Oak (*Quercus velutina*)	Blackjack Oak (*Q. marilandica*)
		Blackgum (*Nyssa sylvatica*)	Shortleaf Pine (*P. echinata*)	White Oak (*Q. alba*)	Scrub Oak (*Q. ilicifolia*)
		Sweetbay Magnolia (*Magnolia virginiana*)	Virginia Pine (*P. virginiana*)	Chestnut Oak (*Q. prinus*)	Swamp White Oak (*Q. bicolor*)
		Gray Birch (*Betula populifolia*)	Loblolly Pine (*P. taeda*)	Post Oak (*Q. stellata*)	
		American Elm (*Ulmus americana*)		Southern Red Oak (*Q. falcata*)	
		Silver Maple (*Acer saccharinum*)		Scarlet Oak (*Q. coccinea*)	

During the growing season, however, oak and pine inventory points had similar daily ET rates (e.g. Fig. 7).

We found wetland forests to have higher ET rates than uplands. In the same landscape Walker et al. (2011) similarly reported lower ET for uplands compared to wetlands, though measurements occurred only at one point for each, and there was no differentiation as to composition. As here, other coastal plain wetland forests have reported ET values that nearly equal or exceed precipitation (Gholz and Clark, 2002; Sun et al., 2010; Liu et al., 2018) due to the availability of soil moisture and surface ponding during portions of the year. We observed Atlantic white cedar to consistently have the highest average ET rates across all years and months, particularly in the spring (March-May) and late summer (August-September). Other *Chamaecyparis* forests at full stocking achieve high LAI values (Sumida et al., 2018) and achieve higher SDI values than other forest types in this landscape, indicating the importance of stand structural traits associated with different species for high ET rates.

Although wetlands overall had higher ET rates than uplands, when we isolated this comparison to only pitch-pine dominated points we observed only modest differences between upland and lowland using the credible interval approach. This is at least partially due to the difficulty in making a binary distinction of wetland status. For this analysis, we used the LULC15 dataset to determine whether a pixel fell in a wetland. However, the gradual topography and fluctuating water table of this landscape make the distinction between pine upland and lowland blurry. Wetland forest types have water tables closer to the surface but unlike cedar and hardwood swamps, pitch pine lowlands rarely experience ponded water (Laidig et al., 2010). Free evaporation from standing water is less likely for pitch pine lowlands, so the increase in ET probably has to do with more available soil water and the longer-term increase in forest occupancy it has permitted.

Some of our results pointed to the importance of forest structural characteristics in driving ET and not only landscape position or cover type. In the conifer-dominated forest types, upland forest identified as having higher canopy cover had higher annual ET. For the extensive coniferous forest types more crown cover was associated with a 7% increase in annual ET (Table 6), and a nearly 4% increase in mixed forests

Table A2
Extent of land cover classes in state forests and study area landscape.

Land use class	Anderson LULC code	Extent in Wharton & Brendan T Byrne state forests (ha)	Extent in study area landscape (ha)
Coniferous Forest (>50% Crown Closure)	4220	16733	72589
Coniferous Wooded Wetlands	6220	7250	23745
Mixed Forest (>50% Coniferous with >50% Crown Closure	4312	6887	28583
Mixed Forest (>50% Deciduous with >50% Crown Closure	4322	4866	26251
Atlantic White Cedar Wetlands	6221	4158	15192
Mixed Forested Wetlands (Coniferous Dominant)	6252	2991	17277
Coniferous Forest (10-50% Crown Closure)	4210	2947	22823
Deciduous Wooded Wetlands	6210	2557	50729
Deciduous Forest (>50% Crown Closure)	4120	1861	42209
Mixed Forested Wetlands (Deciduous Dominant)	6251	1435	12878

dominated by conifers. In contrast, the deciduous forest types had a slightly lower annual ET with higher crown cover: deciduous forests showed a 4% decrease in ET with higher cover, while mixed deciduous-dominated forests showed a 2% decrease. Inference around the open-canopy deciduous forest types is not as strong, however, as these had the smallest sample sizes of the upland land use categories we considered, representing only 34 hectares of open canopy deciduous forest and 115 hectares of mixed deciduous-dominated forest. The most extensive upland forest cover type, coniferous forest with >50% canopy cover, covered more than 11,000 hectares in our analyses. Overall, our results indicate that increased canopy cover is strongly linked to increased annual ET in coniferous-dominated forest in this region.

More evidence for the importance of structural characteristics in driving annual ET rates comes from the model parameters in Tables 4 and 6. Though there was no cover parameter in model A4, the 'Plot' and 'Pixel' random effects in models A4 and B6, respectively, encompass greater residual variation than the random effects of the year or the model residual. We interpreted this result to mean that the between-plot effect size ('plot' and 'pixel' random effects) was greater than the variability introduced by annual variation ('year' random effect) or the model residual variation ('residual' random effect within each plot). This implies that there are differences between pixels of the same forest type or forest cover that have a greater effect on ET rates than indicated by the effect of annual variation or within-plot model residuals. At broad scales, changes in forest structural characteristics (e.g. biomass) were shown by Jaramillo et al. (2018) to better explain residuals in ET and hydroclimatic change than did changes in forest area or composition, demonstrating the significance of forest structure in hydrological ecosystem services. Our results provide a foundation to further examine how differences within forest types, such as forest stocking, site quality, or other variables may influence ET.

4.3. Effects of management

4.3.1. Thinning

For our purposes, we defined "thinning" as any forest cutting meant to concentrate site growth in the remaining trees. In this region, most thinning was either thinning-from-below or a variant of variable-density thinning (McIntyre et al., 2008). Residual basal area post-thinning was usually around 13.8-18.4 m^2 ha^{-1} (60-80 ft^2 $acre^{-1}$), down from levels around 23-27.6 m^2 ha^{-1} (100-120 ft^2 ac^{-1}) or higher. In portions of sites thinned with variable-density methods, some areas were cut to as low as 6.9 m^2 ha^{-1} (30 ft^2 ac^{-1}), a feature designed to spur regeneration in small, dispersed patches. These, however, represented the extreme low-end of the distribution of residual BA and occurred only in the less-common variable-density thinned sites. Overall, thinning activities left the majority of canopy intact and resulted in only a modest reduction in site occupancy. Such moderate disturbance to the canopy structure caused a moderate, medium-duration reduction in ET in our study.

Previous work on the effects of thinning on ET had greater resolution on the intensity of individual treatments but did not characterize changes in ET beyond 1-3 years post-thinning. Liu et al. (2018) observed that reduction in ET had disappeared by the third year, with row/-selection thinning that removed >50% of basal area from the larger diameter size classes in a coastal plain loblolly pine plantation. Grace et al. (2006) observed higher water yield in the year following row thinning in a young loblolly pine plantation. In arid ponderosa pine forests Dore et al. (2010) observed a 10% reduction in annual ET in the first year following a thinning-from-below that removed 1/3 of basal area. Baker (1986), also working in Ponderosa pine stands, observed that the streamflow effects of strip thinning lasted less than three years, although topographic position and aspect played an important role in determining effects. Following pre-commercial thinning on balsam fir and tamarack wetland sites, Jutras et al. (2006) observed 1-2 years of rising water table from thinning-induced reduction in ET. Similarly, Gebhardt et al. (2014) observed reduced stand ET in both moderate and heavy thinning (43% and 70% reduction in BA, respectively) into the third-year post-cut for Norway spruce stands. In contrast, Skubel et al. (2015) observed no decrease in annual ET for the first-year post-thinning in a mature temperate pine forest, but in that case characterized a low thinning where the proportion of basal area removed was approximately 10%, smaller than thinning levels in other studies. Some of the increased duration of ET effects that we observed could be due to the inclusion of the more significant variable-density thinning as it removes more trees whose crown make larger contributions to canopy leaf area, but selection criteria for trees to be removed varies in other studies. Our method substituted reduced precision in evaluating growing space changes for increased temporal resolution over the duration of all thinning activities.

The rate of ET recovery in thinned areas is reflective of stand conditions and the rate at which residual trees increase individual growth and capture newly available resources. After a thinning, trees and saplings that take advantage of increased water availability are already present. We observed a somewhat longer duration of effect of thinning on ET than other studies in coastal pine forests (Liu et al., 2018), but this likely has to do with the contrast in site conditions and management practices employed in other studies and those in our study area. Trees in the commercial sites observed elsewhere are managed to re-occupy vacated growing space as rapidly as possible to realize economic gain. As well, fertilizer and improved genetic stock are used in commercially-managed sites, in part to quickly re-occupy vacated growing space. Importantly, thinning in commercial sites is timed to occur when the residual trees still have vigorous enough growth (ample root zones, larger live crown ratios, etc.) to rapidly take advantage of available space. In contrast, tree growth rates are mostly unmanaged in this area. The regulatory body for forest management in the New Jersey Pinelands prohibits the use of fertilizer and most varieties of improved seedlings (New Jersey Pinelands Commission, 2020), so these factors are not currently important in our study area. Thinning for fuel reduction, a major application in our study area, places lower priority on the growth response of residual trees. These factors are likely responsible for some of the slower recovery ET following thinning that we observed.

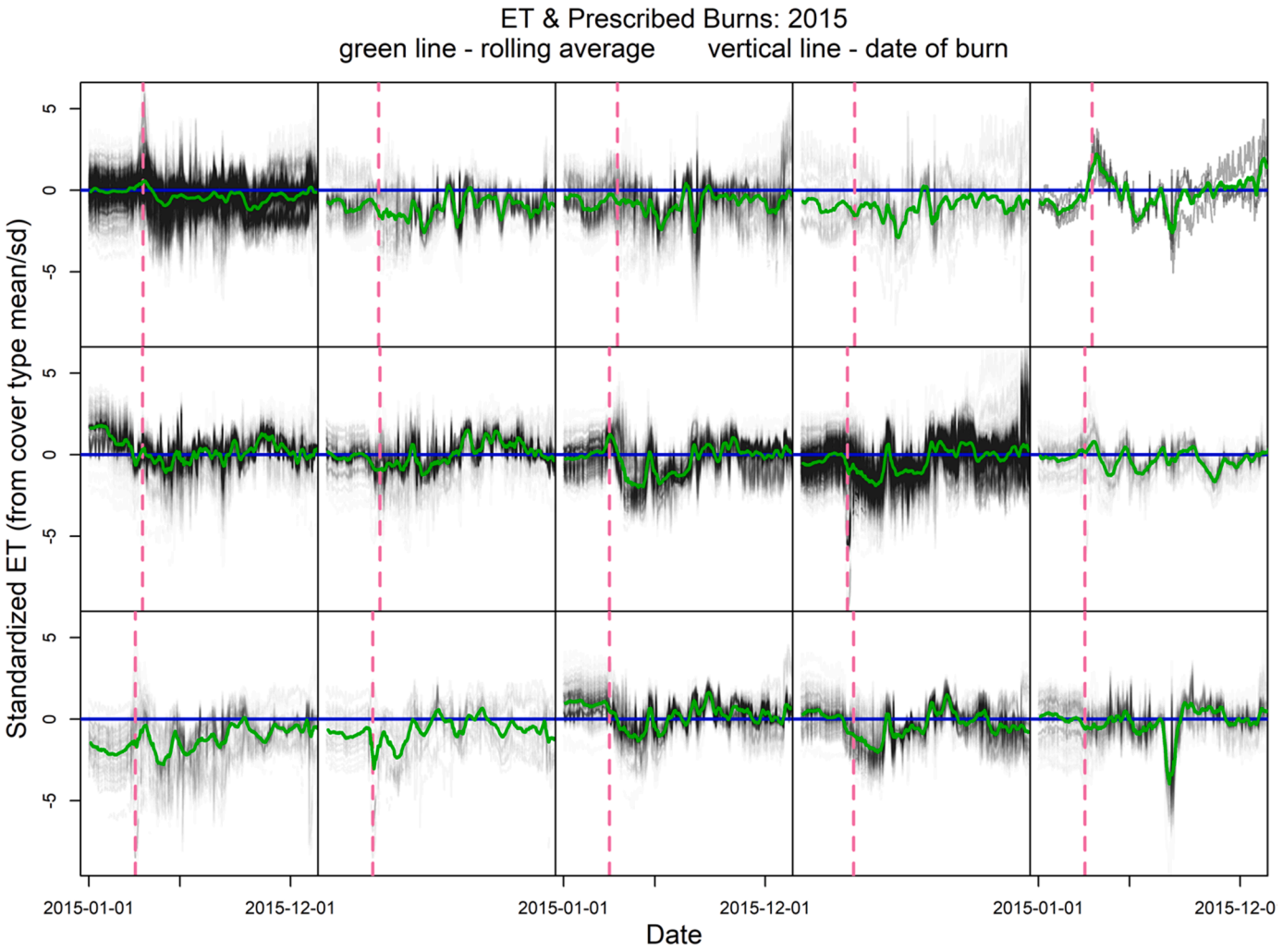


Fig. B1. Line concentration plots of the effect of individual prescribed fires on evapotranspiration for the year 2015. Each panel represents a single burn block. Each semi-transparent line represents the daily z-score for a single pixel, calculated as the daily ET for that pixel minus the mean daily ET for that cover type, divided by the daily standard deviation of ET for that cover type. Green lines are 7-day rolling averages, vertical broken lines are dates of burn. (For interpretation of the references to color in this figure legend, the reader is referred to the web version of this article.)

4.3.2. *Seed tree harvest*

Sites regenerated through seed tree harvests experienced a longer duration of reduced ET than thinned sites, with a slower recovery rate and a larger absolute reduction (Figs. 9, and 11). We interpreted this to be the result of these sites needing new trees to be established before they can grow into vacated growing space. Most of the seed tree harvests in this area left similar residuals: large, vigorous pitch and shortleaf pines, with a total residual basal area of <3.4 m^2 ha^{-1} (<15 ft^2 $acre^{-1}$). The new generation of trees on these sites was usually a mix of plantings and natural regeneration of native pine species. Sites were often planted with seedlings, but residual trees, neighboring stands, and the existing seed bank stimulated additional natural regeneration. In many cases there was additional site preparation post-harvest to kill competing vegetation, such as drum-chopping or dispersing whole-tree chip skid trails throughout a site. This would additionally depress ET rates as existing shrubs and seedlings would not be available on site to grow into vacated space. Conversely, such preparation is usually used to speed the capture of the site by trees by eliminating competition. We did not attempt to partition the effect on ET of each step in the harvest (cutting overstory, moving material, site preparation, planting) as we did not have high-temporal or sub-stand spatial resolution information on the progress of each management activity, though the DisALEXI method would otherwise make this possible. The duration of the ET anomaly for regeneration harvests (seed tree cuts, here) of approximately 13 years was consistent with the duration of decreased ET observed by Sun et al. (2008) and Aguilos et al. (2021), and corresponded with the duration of increased streamflow observed by Verry (1986), but was faster than recovery in ET observed by Ford et al. (2011) and Komatsu et al. (2008), and slower than in Gholz and Clark (2002) for slash pine plantations. As with thinning in other locations, faster recovery following regeneration treatments in some systems is the purposeful result of active management intended to recover LAI rapidly and ensure maximum growing space occupancy.

4.3.3. *Prescribed fire*

The mild but somewhat variable effect in site response after prescribed burning aligns with the applications of prescribed burning in this study area. Fire is intentionally applied to this landscape only when very tightly controlled conditions exist, as the weather must be within the prescription and within the seasonal window allowed by state policy. Prescribed burns must occur between October 15th and March 31st (with few exceptions); in the study area understory vegetation are largely dormant during this period. Additionally, air temperature is typically between 0 and 15 °C, with relative humidity between 30-60% and winds no more than 9 m s^{-1}. For most of the burns applied during 2015-2017, these requirements precluded most overstory mortality from fire so that

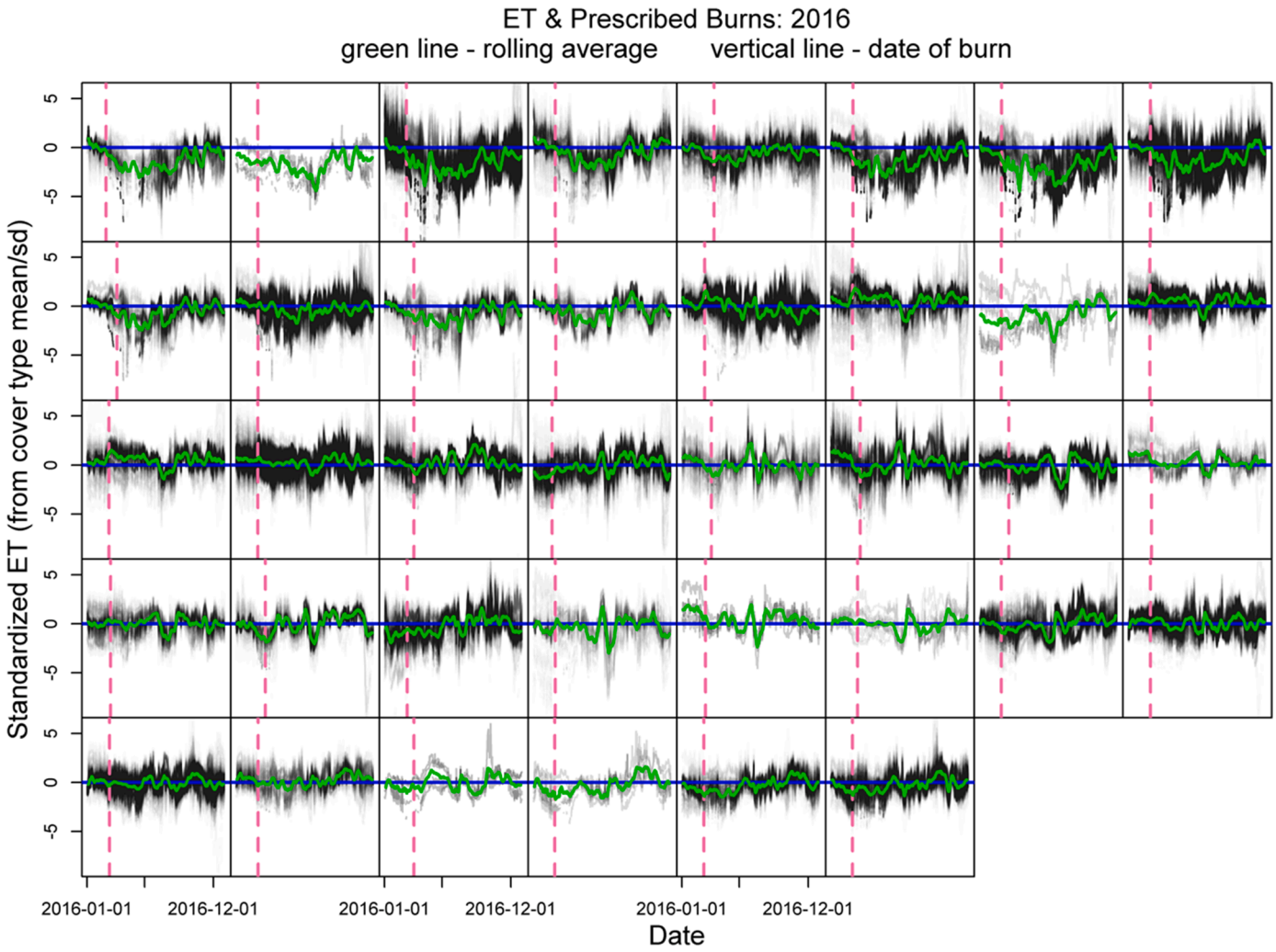


Fig. B2. Line concentration plots of the effect of individual prescribed fires on evapotranspiration for the year 2016. Each panel represents a single burn block. Each semi-transparent line represents the daily z-score for a single pixel, calculated as the daily ET for that pixel minus the mean daily ET for that cover type, divided by the daily standard deviation of ET for that cover type. Green lines are 7-day rolling averages, vertical broken lines are dates of burn. (For interpretation of the references to color in this figure legend, the reader is referred to the web version of this article.)

there was little significant structural change to burned areas. In hotter fires, buoyant heat plumes killed some of the existing canopy foliage, but the spring flush of growth restored leaf tissue shortly thereafter. Only in the most intense prescribed burns was needle mortality or branch dieback sufficient to cause lingering effects on ET (e.g. Figs. 14 & 15).

Instead, prescribed fire's effects on ET, like cutting, was dependent on the purpose of the activity. Where the burn boss intended to kill some overstory stems, ET impacts persisted for as long as a few growing seasons. For the vastly more common application of prescribed fire, with the fire intended to reduce surface fuel loading to decrease wildfire risks but not kill overstory, modest reductions in stand-level ET lasted less than the duration of a single growing season. Initially, this seems to contrast with Renninger et al. (2013), who observed a short decrease but then increased transpiration and photosynthetic rates across all tree diameter classes of pitch pine following a prescribed fire. Increased tree ET in that case was likely caused by reduced competition from shrubs as well higher LAI from the fertilizing effect of pyromineralization by the prescribed fire. Using eddy covariance in the same landscape, Clark et al. (2014) found that prescribed fires reduced stand ET in the first few months but had only a minor effect at the annual scale, with variability being more driven by precipitation or the presence of insect damage.

5. Conclusion

Application of the DisALEXI model in the forested coastal plain landscape of southern New Jersey provides a detailed and promising approach to the characterization of ET. We consistently observed differences in forest ET from forest composition and canopy cover and used these differences to better characterize the effects of forest management on ET. There was a variable effect of management on water yield, where the intensity and duration of the ET anomaly was qualitatively related to the intensity of overstory disturbance. These findings and model components suggest that it should be possible to establish a relationship between some metrics of forest occupancy and forest ET across this landscape. Our results also provide temporal resolution to quantifying the effects of some common forest management practices on ET. This will improve the parameterizing of models that quantify changes in hydrologic ecosystem services, particularly given the importance of water provisioning in this landscape.

Our results suggest that landscape-scale changes in forest canopy cover, forest composition, and forest disturbances will play an important role in regional water management. These factors play a significant role in stand ET and the water budgets because they impact the dominant land cover across the region. When experienced at scale, subtle changes in these attributes may have significant regional-scale effects.

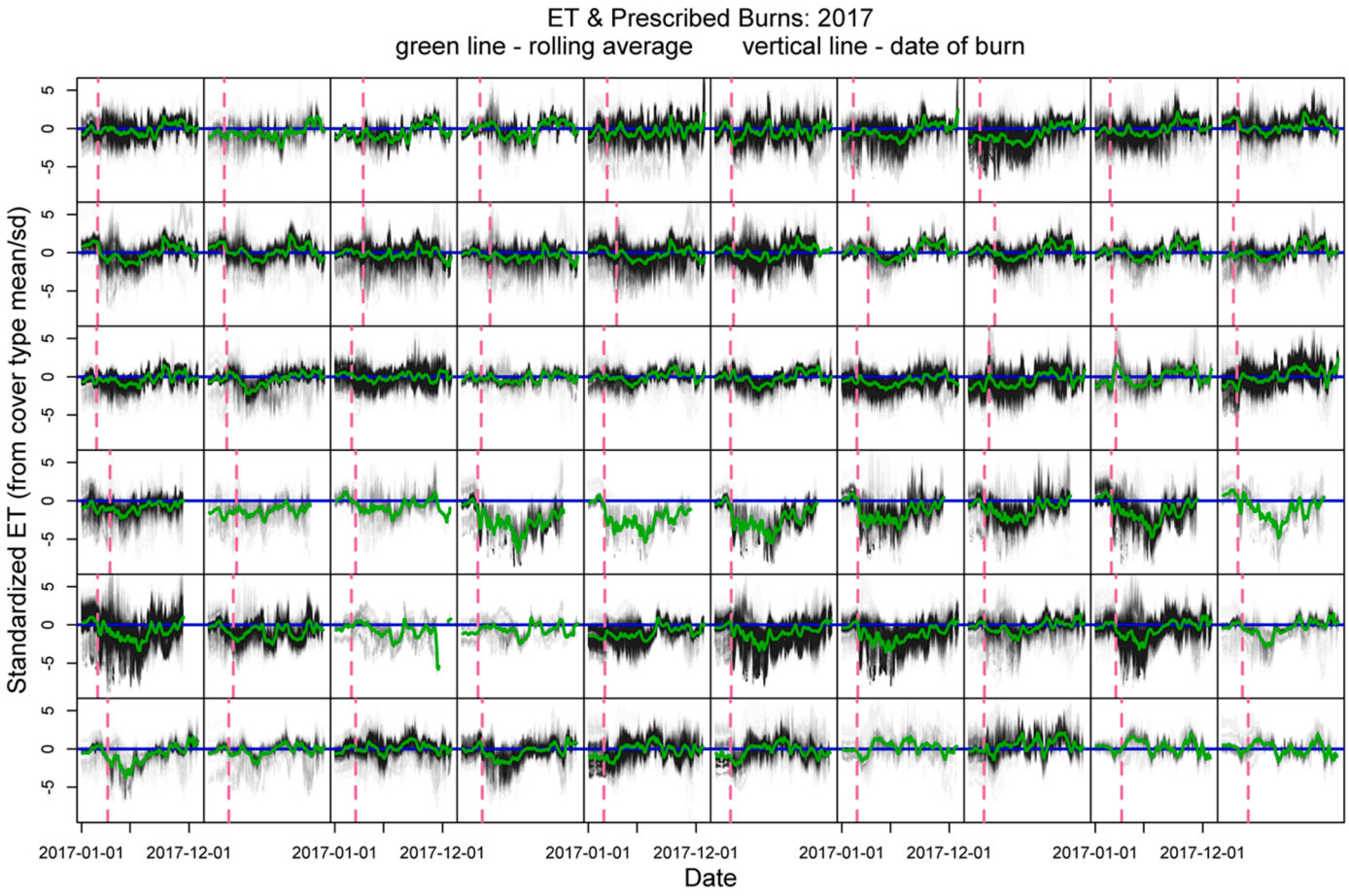


Fig. B3. Line concentration plots of the effect of individual prescribed fires on evapotranspiration for the year 2017. Each panel represents a single burn block. Each semi-transparent line represents the daily z-score for a single pixel, calculated as the daily ET for that pixel minus the mean daily ET for that cover type, divided by the daily standard deviation of ET for that cover type. Green lines are 7-day rolling averages, vertical broken lines are dates of burn. (For interpretation of the references to color in this figure legend, the reader is referred to the web version of this article.)

Declaration of Competing Interest

The authors declare that they have no known competing financial interests or personal relationships that could have appeared to influence the work reported in this paper.

Data availability

Data will be made available on request.

Acknowledgements

This research was conducted with financial support from NIFA McIntire Stennis grant NJ17318 and the John and Eleanor Kuser endowment in urban and community forestry. This work was also supported by the New Jersey Department of Environmental Protection Forest Service, the United States Department of Agriculture – Agricultural Research Service and NASA ECOSTRESS program (Grant Number: 80NSSC23K0642). The authors wish to acknowledge the support of the Rutgers Center for Remote Sensing and Spatial Analysis for their computational support. Many thanks also to William Zipse, Rosa Yoo, and Courtney Willitts for supporting the state data streams. We thank our anonymous reviewer for their thoughtful, constructive, and useful feedback – it really strengthened the quality of the paper.

Appendix A. Forest Inventory & Land Use Data Summaries

Appendix B. Individual Prescribed Burn Effects

References

Aguilos, M., Sun, G., Noormets, A., Domec, J.-C., McNulty, S., Gavazzi, M., Prajapati, P., Minick, K.J., Mitra, B., King, J., 2021. Ecosystem productivity and evapotranspiration are tightly coupled in loblolly pine (Pinus taeda L.) plantations along the coastal plain of the Southeastern U.S. Forests 12, 1123. https://doi.org/10.3390/f12081123.

Anderson, M., Gao, F., Knipper, K., Hain, C., Dulaney, W., Baldocchi, D., Eichelmann, E., Hemes, K., Yang, Y., Medellin-Azuara, J., Kustas, W., 2018. Field-scale assessment of land and water use change over the California delta using remote sensing. Remote Sens. 10, 889. https://doi.org/10.3390/rs10060889.

Anderson, M.C., Norman, J.M., Diak, G.R., Kustas, W.P., Mecikalski, J.R., 1997. A two-source time-integrated model for estimating surface fluxes using thermal infrared remote sensing. Remote Sens. Environ. 60, 195–216. https://doi.org/10.1016/S0034-4257(96)00215-5.

Anderson, M.C., Norman, J.M., Kustas, W.P., Houborg, R., Starks, P.J., Agam, N., 2008. A thermal-based remote sensing technique for routine mapping of land-surface carbon, water and energy fluxes from field to regional scales. Remote Sens. Environ. 112, 4227–4241. https://doi.org/10.1016/j.rse.2008.07.009.

Anderson, M.C., Norman, J.M., Mecikalski, J.R., Otkin, J.A., Kustas, W.P., 2007. A climatological study of evapotranspiration and moisture stress across the continental United States based on thermal remote sensing: 1. Model formulation. J. Geophys. Res. 112 https://doi.org/10.1029/2006JD007506.

Anderson, M.C., Norman, J.M., Mecikalski, J.R., Torn, R.D., Kustas, W.P., Basara, J.B., 2004. A multiscale remote sensing model for disaggregating regional fluxes to

micrometeorological scales. J. Hydrometeorol. 5, 343–363. https://doi.org/10.1175/1525-7541(2004)005<0343:AMRSMF>2.0.CO;2.
Baker Jr., M.B., 1986. Effects of ponderosa pine treatments on water yield in Arizona. Water Resour. Res. 22, 67–73. https://doi.org/10.1029/WR022i001p00067.
Bates, D., Mächler, M., Bolker, B., Walker, S., 2015. Fitting linear mixed-effects models using lme4. J. Stat. Softw. 67, 1–48. https://doi.org/10.18637/jss.v067.i01.
Baty, F., Ritz, C., Charles, S., Brutsche, M., Flandrois, J.-P., Delignette-Muller, M.-L., 2015. A toolbox for nonlinear regression in r: the package nlstools. J. Stat. Softw. 66, 1–21. https://doi.org/10.18637/jss.v066.i05.
Beamesderfer, E.R., Arain, M.A., Khomik, M., Brodeur, J.J., Burns, B.M., 2020. Response of carbon and water fluxes to meteorological and phenological variability in two eastern North American forests of similar age but contrasting species composition – a multiyear comparison. Biogeosciences 17, 3563–3587. https://doi.org/10.5194/bg-17-3563-2020.
Bivand, R., Keitt, T., Rowlingson, B., 2022. rgdal: Bindings for the "Geospatial" Data Abstraction Library.
Borchers, H.W., 2022. pracma: Practical Numerical Math Functions.
Bosch, J.M., Hewlett, J.D., 1982. A review of catchment experiments to determine the effect of vegetation changes on water yield and evapotranspiration. J. Hydrol. 55, 3–23. https://doi.org/10.1016/0022-1694(82)90117-2.
Brown, T.C., Hobbins, M.T., Ramirez, J.A., 2008. Spatial distribution of water supply in the coterminous United States [1]. J. Am. Water Resour. Assoc. 44, 1474–1487. https://doi.org/10.1111/j.1752-1688.2008.00252.x.
Burba, G., 2013. Eddy Covariance Method. LI-COR Biosciences.
Clark, K.L., 2016. AmeriFlux US-Slt Silas Little- New Jersey. Ver. 5-1.
Clark, K.L., Skowronski, N., Gallagher, M., Renninger, H., Schäfer, K., 2012. Effects of invasive insects and fire on forest energy exchange and evapotranspiration in the New Jersey pinelands. Agric. For. Meteorol. 166–167, 50–61. https://doi.org/10.1016/j.agrformet.2012.07.007.
Clark, K.L., Skowronski, N.S., Gallagher, M.R., Renninger, H., Schäfer, K.V.R., 2014. Contrasting effects of invasive insects and fire on ecosystem water use efficiency. Biogeosciences 11, 6509–6523. https://doi.org/10.5194/bg-11-6509-2014.
Crocker, S.J., Barnett, C.J., Butler, B.J., Hatfield, M.A., Kurtz, C.M., Lister, T.W., Meneguzzo, D.M., Miles, P.D., Morin, R.S., Nelson, M.D., Piva, R.J., Reimann, R., Smith, J.E., Woodall, C.W., Zipse, W., 2017. New Jersey Forests 2013 (No. NRS-RB-109). U.S. Department of Agriculture, Forest Service, Northern Research Station. Newtown Square, PA. https://doi.org/10.2737/NRS-RB-109.
Dixon, G., Keyser, C., 2019. Forest Vegetation Simulator: Northeast (NE) Variant Overview.
Dore, S., Kolb, T.E., Montes-Helu, M., Eckert, S.E., Sullivan, B.W., Hungate, B.A., Kaye, J. P., Hart, S.C., Koch, G.W., Finkral, A., 2010. Carbon and water fluxes from ponderosa pine forests disturbed by wildfire and thinning. Ecol. Appl. 20, 663–683. https://doi.org/10.1890/09-0934.1.
Douglass, J.E., Swank, W.T., 1972. Streamflow modification through management of eastern forests. In: Res. Pap. SE-94, 17. U.S. Department of Agriculture, Forest Service, Southeastern Forest Experiment Station, Asheville, NC, p. 094.
Elzhov, T.V., Mullen, K.M., Spiess, A.-N., Bolker, B., 2022. minpack.lm: R Interface to the Levenberg-Marquadt Nonlinear Least=Squares Algorithm Found in MINPACK. Plus Support for Bounds.
Ex, S.A., Smith, F.W., 2013. Stand density index estimates leaf area index in uneven-aged ponderosa pine stands. Western J. Appli. For. 28, 9–12. https://doi.org/10.5849/wjaf.12-004.
Ford, C.R., Hubbard, R.M., Kloeppel, B.D., Vose, J.M., 2007. A comparison of sap flux-based evapotranspiration estimates with catchment-scale water balance. Agric. For. Meteorol. 145, 176–185. https://doi.org/10.1016/j.agrformet.2007.04.010.
Ford, C.R., Laseter, S.H., Swank, W.T., Vose, J.M., 2011. Can forest management be used to sustain water-based ecosystem services in the face of climate change? Ecol. Appl. 21, 2049–2067. https://doi.org/10.1890/10-2246.1.
Freshwater, 1987. Wetlands Protection Act. New Jersey Statutes Ann, p. 9B. §13.
Galloway Township, Rev. Ordinances Art. VII §233-52 (2006).
Gao, F., Masek, J., Schwaller, M., Hall, F., 2006. On the blending of the Landsat and MODIS surface reflectance: predicting daily Landsat surface reflectance. IEEE Trans. Geosci. Remote Sens. 44, 2207–2218. https://doi.org/10.1109/TGRS.2006.872081.
Garcia-Prats, A., del Campo, A.D., Pulido-Velazquez, M., 2016. A hydroeconomic modeling framework for optimal integrated management of forest and water. Water Resour. Res. 52, 8277–8294. https://doi.org/10.1002/2015WR018273.
Gebhardt, T., Häberle, K.-H., Matyssek, R., Schulz, C., Ammer, C., 2014. The more, the better? Water relations of Norway spruce stands after progressive thinning. Agric. For. Meteorol. 197, 235–243. https://doi.org/10.1016/j.agrformet.2014.05.013.
Gholz, H.L., Clark, K.L., 2002. Energy exchange across a chronosequence of slash pine forests in Florida. Agric. For. Meteorol. 112, 87–102. https://doi.org/10.1016/S0168-1923(02)00059-X.
Grace, J.M., Skaggs, R.W., Chescheir, G.M., 2006. Hydrologic and water quality effects of thinning loblolly pine. Trans. ASABE 49, 645–654.
Hewes, J.H., Butler, B.J., Liknes, G.C., Nelson, M.D., Snyder, S.A., 2014. Map of Distribution of Six Forest Ownership Types in the Conterminous United States (No. NRS-RMAP-6). U.S. Department of Agriculture, Forest Service, Northern Research Station, Newtown Square, PA. https://doi.org/10.2737/NRS-RMAP-6.
Hijmans, R.J., 2022. raster: Geographic Data Analysis and Modeling.
Jackson Township, Rev. Ordinances Part II §405 (2009).
Jaramillo, F., Cory, N., Arheimer, B., Laudon, H., van der Velde, Y., Hasper, T.B., Teutschbein, C., Uddling, J., 2018. Dominant effect of increasing forest biomass on evapotranspiration: interpretations of movement in Budyko space. Hydrol. Earth Syst. Sci. 22, 567–580. https://doi.org/10.5194/hess-22-567-2018.
Jutras, S., Plamondon, A.P., Hökkä, H., Bégin, J., 2006. Water table changes following precommercial thinning on post-harvest drained wetlands. For. Ecol. Manag. 235, 252–259. https://doi.org/10.1016/j.foreco.2006.08.335.
Knipper, K.R., Kustas, W.P., Anderson, M.C., Nieto, H., Alfieri, J.G., Prueger, J.H., Hain, C.R., Gao, F., McKee, L.G., Alsina, M.M., Sanchez, L., 2020. Using high-spatiotemporal thermal satellite ET retrievals to monitor water use over California vineyards of different climate, vine variety and trellis design. Agric. Water Manage. 241, 106361 https://doi.org/10.1016/j.agwat.2020.106361.
Komatsu, H., Kume, T., Otsuki, K., 2008. The effect of converting a native broad-leaved forest to a coniferous plantation forest on annual water yield: A paired-catchment study in northern Japan. For. Ecol. Manag. 255, 880–886.
Laidig, K.J., Zampella, R.A., Brown, A.M., Procopio, N.A., 2010. Development of vegetation models to predict the potential effect of groundwater withdrawals on forested wetlands.
Liu, X., Sun, G., Mitra, B., Noormets, A., Gavazzi, M.J., Domec, J.-C., Hallema, D.W., Li, J., Fang, Y., King, J.S., McNulty, S.G., 2018. Drought and thinning have limited impacts on evapotranspiration in a managed pine plantation on the southeastern United States coastal plain. Agric. For. Meteorol. 262, 14–23. https://doi.org/10.1016/j.agrformet.2018.06.025.
McIntyre, R.K., Jack, S.B., Mitchell, R.J., Hiers, J.K., Neel, W.L., 2008. Multiple Value Management: The Stoddard-Neel Approach to Ecological Forestry in Longleaf Pine Grasslands.
McLaughlin, D.L., Kaplan, D.A., Cohen, M.J., 2013. Managing forests for increased regional water yield in the Southeastern U.S. coastal plain. J. Am. Water Resour. Assoc. 49, 953–965. https://doi.org/10.1111/jawr.12073.
Moffat, A.M., Papale, D., Reichstein, M., Hollinger, D.Y., Richardson, A.D., Barr, A.G., Beckstein, C., Braswell, B.H., Churkina, G., Desai, A.R., Falge, E., Gove, J.H., Heimann, M., Hui, D., Jarvis, A.J., Kattge, J., Noormets, A., Stauch, V.J., 2007. Comprehensive comparison of gap-filling techniques for eddy covariance net carbon fluxes. Agric. For. Meteorol. 147, 209–232. https://doi.org/10.1016/j.agrformet.2007.08.011.
National Parks and Recreation Act of 1978. Public Law 95-625; 16 U.S.C. 471i (1978).
New Jersey Department of Environmental Protection, 2019. Land Use/Land Cover of New Jersey 2015 [WWW Document]. https://gisdata-njdep.opendata.arcgis.com/datasets/6f76b90deda34cc98aec255e2defdb45.
New Jersey Legislature, 1961. New Jersey Statutes Ann. §13:1B-15.5.
New Jersey Pinelands Commission, 2020. Comprehensive Management Plan [WWW Document]. https://www.nj.gov/pinelands/cmp/. accessed 3.12.21.
Norman, J.M., Anderson, M.C., Kustas, W.P., French, A.N., Mecikalski, J., Torn, R., Diak, G.R., Schmugge, T.J., Tanner, B.C.W., 2003. Remote sensing of surface energy fluxes at 10-m pixel resolutions. Water Resour. Res. 39 https://doi.org/10.1029/2002WR001775.
Norman, J.M., Kustas, W.P., Humes, K.S., 1995. Source approach for estimating soil and vegetation energy fluxes in observation of directional radiometric surface temperature. Agric. For. Meteorol. 77, 263–293.
Ocean Township, 1989. Rev. Ordinances Part II 373. §.
Ovando, P., Brouwer, R., 2019. A review of economic approaches modeling the complex interactions between forest management and watershed services. For. Policy Econ. 100, 164–176. https://doi.org/10.1016/j.forpol.2018.12.007.
Pebesma, E.J., Bivand, R.S., 2005. Classes and methods for spatial data in R. R News 5.
Pinelands Protection Act, New Jersey Statutes Ann. § 13:18A (1979).
Renninger, H.J., Clark, K.L., Skowronski, N., Schäfer, K.V.R., 2013. Effects of a prescribed fire on water use and photosynthetic capacity of pitch pines. Trees 27 (4), 1115–1127. https://doi.org/10.1007/s00468-013-0861-5, 27, 1115–1127.
Runkle, J., Kunkel, K., Champion, S., Frankson, R., Stewart, B., Sweet, W., 2017. New Jersey State Climate Summary. NOAA Technical Report NESDIS 149-NJ.
Running, S., Mu, Q., Zhao, M., 2017. MOD16A2 MODIS/Terra Net Evapotranspiration 8-Day L4 Global 500m SIN Grid V006. 10.5067/MODIS/MOD16A2.006.
Schäfer, K.V.R., Renninger, H.J., Clark, K.L., Medvigy, D., 2014. Hydrological responses to defoliation and drought of an upland oak/pine forest: forest water balance under drought and disturbance. Hydrol. Process. 28, 6113–6123. https://doi.org/10.1002/hyp.10104.
Simonit, S., Connors, J.P., Yoo, J., Kinzig, A., Perrings, C., 2015. The impact of forest thinning on the reliability of water supply in Central Arizona. PLoS One 10, e0121596. https://doi.org/10.1371/journal.pone.0121596.
Skubel, R., Arain, M.A., Peichl, M., Brodeur, J.J., Khomik, M., Thorne, R., Trant, J., Kula, M., 2015. Age effects on the water-use efficiency and water-use dynamics of temperate pine plantation forests. Hydrol. Processes 29, 4100–4113. https://doi.org/10.1002/hyp.10549.
Sloto, R.A., Buxton, D.E., 2005. Water budgets for selected watersheds in the Delaware River basin, eastern Pennsylvania and western New Jersey (USGS Numbered Series No. 2005–5113). Water budgets for selected watersheds in the Delaware River basin, eastern Pennsylvania and western New Jersey. Scientific Investigations Report. U.S. Geological Survey. https://doi.org/10.3133/sir20055113.
Spiess, A.-N., 2018. propagate: Propagation of Uncertainty.
State Parks and Forestry, 1983. Resource Act, New Jersey Statutes Ann, 13, p. 1L. §.
Stednick, J., 1996. Monitoring the effects of timber harvest on annual water yield. J. Hydrol. 176, 79–95.
Sumida, A., Watanabe, T., Miyaura, T., 2018. Interannual variability of leaf area index of an evergreen conifer stand was affected by carry-over effects from recent climate conditions. Sci. Rep. 8, 13590. https://doi.org/10.1038/s41598-018-31672-3.
Sumner, D.M., Nicholson, R.S., Clark, K.L., 2012. Measurement and Simulation of Evapotranspiration at a Wetland Site in the New Jersey Pinelands 44.
Sun, G., Caldwell, P.V., McNulty, S.G., 2015. Modelling the potential role of forest thinning in maintaining water supplies under a changing climate across the

conterminous United States. Hydrol. Processes 29, 5016–5030. https://doi.org/10.1002/hyp.10469.
Sun, G., Noormets, A., Chen, J., McNulty, S.G., 2008. Evapotranspiration estimates from eddy covariance towers and hydrologic modeling in managed forests in Northern Wisconsin. Agric. For. Meteorol. 148, 257–267.
Sun, G., Noormets, A., Gavazzi, M.J., McNulty, S.G., Chen, J., Domec, J.-C., King, J.S., Amatya, D.M., Skaggs, R.W., 2010. Energy and water balance of two contrasting loblolly pine plantations on the lower coastal plain of North Carolina. For. Ecol. Manage. 259, 1299–1310. https://doi.org/10.1016/j.foreco.2009.09.016.
Sun, G., Zhang, L., Duan, K., Rau, B., 2016. Impacts of forest biomass removal on water yield across the United States, in: 2016 Billion Ton Report.
Swank, W.T., Douglass, J.E., 1974. Streamflow greatly reduced by converting deciduous hardwood stands to pine. Science 185, 857–859.
USDA Forest Service, 2018. Forest Health Mapping & Reporting: Detection Surveys [WWW Document]. https://www.fs.fed.us/foresthealth/applied-sciences/mapping-reporting/detection-surveys.shtml (accessed 3.4.21).
Verry, E.S., 1986. Forest harvesting and water: the lake states experience1. J. Am. Water Resour. Assoc. 22, 1039–1047. https://doi.org/10.1111/j.1752-1688.1986.tb00775.x.
Vose, J.M., Sun, G., Ford, C.R., Bredemeier, M., Otsuki, K., Wei, X., Zhang, Z., Zhang, L., 2011. Forest ecohydrological research in the 21st century: what are the critical needs? Ecohydrology 4, 146–158. https://doi.org/10.1002/eco.193.
Walker, R.L., Nicholson, R.S., Storck, D.A., 2011. Hydrologic assessment of three drainage basins in the Pinelands of southern New Jersey, 2004-06 (USGS Numbered Series No. 2011–5056). Hydrologic assessment of three drainage basins in the Pinelands of southern New Jersey, 2004-06. Scientific Investigations Report. U.S. Geological Survey, Reston, VA. https://doi.org/10.3133/sir20115056.
Water supply management act. N. Jersey Statut. Ann. 58, 1981, 1A.
Woods, A.J., Omernik, J.M., Moran, B.C., 2007. Level III and IV Ecoregions of New Jersey. U.S. Environmental Protection Agency. National Health and Environmental Effects Research Laboratory, Corvallis, OR.
Wulder, M.A., White, J.C., Goward, S.N., Masek, J.G., Irons, J.R., Herold, M., Cohen, W. B., Loveland, T.R., Woodcock, C.E., 2008. Landsat continuity: Issues and opportunities for land cover monitoring. Remote Sens. Environ. 112, 955–969. https://doi.org/10.1016/j.rse.2007.07.004.
Yang, Y., Anderson, M., Gao, F., Hain, C., Noormets, A., Sun, G., Wynne, R., Thomas, V., Sun, L., 2020. Investigating impacts of drought and disturbance on evapotranspiration over a forested landscape in North Carolina, USA using high spatiotemporal resolution remotely sensed data. Remote Sens. Environ. 238, 111018 https://doi.org/10.1016/j.rse.2018.12.017.
Yang, Y., Anderson, M.C., Gao, F., Hain, C.R., Semmens, K.A., Kustas, W.P., Noormets, A., Wynne, R.H., Thomas, V.A., Sun, G., 2017. Daily Landsat-scale evapotranspiration estimation over a forested landscape in North Carolina, USA, using multi-satellite data fusion. Hydrol. Earth Syst. Sci. 21, 1017–1037. https://doi.org/10.5194/hess-21-1017-2017.
Yang, Y., Anderson, M., Gao, F., Hain, C., Wood, J., Gu, L., 2019. Using Daily Stand-Scale Evapotranspiration (ET) Estimated From Remotely Sensed Data to Investigate Drought Impact on ET in a Temporate Forest in the Central Us. In: IGARSS 2019 - 2019 IEEE International Geoscience and Remote Sensing Symposium. Presented at the IGARSS 2019 - 2019 IEEE International Geoscience and Remote Sensing Symposium, pp. 6035–6038. https://doi.org/10.1109/IGARSS.2019.8898301.
Yang, Y., Anderson, M.C., Gao, F., Wood, J.D., Gu, L., Hain, C., 2021a. Studying drought-induced forest mortality using high spatiotemporal resolution evapotranspiration data from thermal satellite imaging. Remote Sens. Environ. 265, 112640 https://doi.org/10.1016/j.rse.2021.112640.
Yang, Y., Anderson, M.C., Gao, F., Johnson, D.M., Yang, Yun, Sun, L., Dulaney, W., Hain, C.R., Otkin, J.A., Prueger, J., Meyers, T.P., Bernacchi, C.J., Moore, C.E., 2021b. Phenological corrections to a field-scale, ET-based crop stress indicator: An application to yield forecasting across the U.S. Corn Belt. Remote Sens. Environ. 257, 112337 https://doi.org/10.1016/j.rse.2021.112337.